REGULATORY INFORMATION DISTRIBUTION SYSTEM (RIDS)

ACCESSION NBR:7812130140 DOC.DATE: 78/12/08 NOTARIZED: NO DOCKET #
FACIL:50-331 DUANE ARNOLD, IOWA ELECTRIC & POWER CO. 05000331
AUTH.NAME AUTHOR AFFILIATION
* IA ELEC LIGHT & PWR
RECIP.NAME RECIPIENT AFFILIATION

SUBJECT: Rept"Duane Arnold Energy Ctr Recirculation Inlet Safe End Repair Prog,781208." Suppl IE Repair Rept submitted on 780731.Repts purpose is to document info presented at 781114 meeting in Cedar Rapids,IA.

DISTRIBUTION CODE: A001S COPIES RECEIVED:LTR __ ENCL __ SIZE:_____
TITLE: GENERAL DISTRIBUTION FOR AFTER ISSUANCE OF OPERATING LIC

NOTES:_____

	RECIPIENT ID CODE/NAME	COPIES LTTR	COPIES ENCL	RECIPIENT ID CODE/NAME	COPIES LTTR	COPIES ENCL
ACTION:	05 BC	7	7			
INTERNAL:	01 REG FILE	1	1	02 NRC PDR	1	1
	12 I&E	2	2	14 HANAUER	1	1
	15 CORE PERF BR	1	1	16 AD SYS/PROJ	1	1
	17 ENGR BR	1	1	18 REAC SFTY BR	1	1
	19 PLANT SYS BR	1	1	20 EEB	1	1
	21 EFLT TRT SYS	1	1	22 BRINKMAN	1	1
EXTERNAL:	03 LPDR	1	1	04 NSIC	1	1
	23 ACRS	16	16			

TOTAL NUMBER OF COPIES REQUIRED: LTTR 38 ENCL 38

DUANE ARNOLD ENERGY CENTER

RECIRCULATION INLET

SAEE END REPAIR PROGRAM

December 8, 1978

INDEX

I	Introduction
II.A	Shutdown
II.B	UT and RT Testing Results
II.C	Safe End Removal
II.D	Cause of Failure
II.E	Status of Remaining Six Safe Ends
II.F	Replacement Design
II.G	Replacement Installation
II.H	Restart Program
II.I	Stress Report
III.A.1	History of Unidentified Leakage
III.A.2	Adequacy of Present Technical Specifications
III.A.3	Leak Before Break
III.A.4	Modifications To Equipment
III.B.1	SwRI Report
III.B.2	GE Evaluation of Cause of Cracking
III.C	Replacement Design
III.C.1	Description
III.C.2	Fabrication
III.C.3	Stress Comparison
III.C.4	Stress Indices
III.C.5	Evaluation of Annulus Flow
III.C.6	Vibration/Hydraulics
III.C.7	Adequacy of Alloy 600
III.C.8.a	Weld Number 3
III.C.8.b	Residual Stress Analysis
III.C.8.c	Mockup
III.C.8.d	Inspections
III.D	Replacement/Installation
III.E.1	Inservice Inspection
III.E.2	Capability of UT
III.E.3	Other Inconel Nozzles
III.E.4	Inspections

I. Introduction

The purpose of this Iowa Electric Light & Power Company (IE) Report is to document the information presented at the N.R.C. Meeting in Cedar Rapids, Iowa on November 14, 1978, concerning the repair program for eight recirculation inlet nozzle safe ends at the Duane Arnold Energy Center (DAEC). This report supplements the IE Repair Report submitted to the N.R.C. on July 31, 1978. Additionally, the Report includes responses to questions raised by the N.R.C. staff at the November 14, 1978 and December 5, 1978 meetings, and a discussion of those steps which will be taken prior to DAEC restart.

This Report presents the chronology of events and methods employed by IE with regard to shutdown of the DAEC in June, 1978, investigation of the monitored unidentified leakage, removal of the defective safe-ends, replacement preparations and techniques, and startup. The initial results of an extensive metallurgical investigation conducted by Southwest Research Institute (SwRI) were reported to the N.R.C. on October 27, 1978. Generally, the SwRI Interim Report concluded that the cause of cracking was intergranular stress corrosion. This interim study will be supplemented by a report to be issued in December, 1978. In addition to the

SwRI laboratory analyses and conclusions, General Electric (GE) has written an in-depth analysis of the cause of cracking of the DAEC safe ends, set forth in Section III.B.2 of this Report. An extensive discussion of the design of the replacement safe-end is also incorporated herein. In the new configuration, the stress levels are greatly reduced, the weld proximate to the cracking in the old safe end has been removed from the pressure boundary, and water will be flushed through the annulus at a rate that prevents the annulus from becoming a crevice, that is, a location of stagnant water. The Report also addresses leak detection and inspection methods to be employed in the future at the DAEC, including ultrasonic testing methods and investigation of other potentially creviced inconel components.

The DAEC will not be operated until the repairs have been completed to the satisfaction of the N.R.C.

II.A Shutdown

The DAEC had been monitoring a slowly increasing drywell unidentified leakage since May 1, 1978. On June 14, 1978 an increase in unidentified leakage was observed. The leakage increased from approximately 1 gpm to approximately 3 gpm during the day of June 14, 1978.

The increased leakage was immediately observed by six independent methods:

1. Control room recorders indicated increased drywell sump pumping activity.
2. Radwaste control room operators noticed increased tank levels.
3. Iodine levels in the drywell increased.
4. Drywell temperature in local areas showed slight increases.
5. Particulate radiation levels increased slightly.
6. Containment atmosphere weight increased.

As is normal for any unexpected increase in drywell leakage, the plant initiated an investigation to determine the possible cause of the increase in leakage. The investigation progress was discussed in meetings during the week. A decision was made late on Friday, June 13 to wait until Monday to see if the leakage would remain

steady. The leakage at that time was about 3.2 gpm in comparison to the technical specification limit of 5.0 gpm.

At 00:55 on June 17, 1978, during weekly control valve testing, an automatic reactor scram occurred due to problems in reactor protection system relays associated with the testing. The Chief Engineer was notified approximately thirty minutes after the shutdown. The Chief Engineer made the decision to reduce reactor pressure, deinert the containment, enter the containment and investigate the leakage. Based on the week's observation of drywell leakage and the fact that the plant was shut down, it seemed prudent to look for the leak rather than wait until the leakage approached the technical specification limit of 5.0 gpm.

The survey of the drywell revealed a leak in the area of the N2A nozzle. The next several hours were spent removing shield blocks and insulation to determine the actual source of the leak. The NRC Region III office was notified of preliminary findings and when the actual source of leakage was identified, the Region III office was notified. This occurred at 13:15 on June 17, 1978. Preparations then began for possible repairs.

II.B Ultrasonic and Radiographic Testing Results

Ultrasonic testing and radiographic examinations were performed to determine the full extent of the cracking in the N2A safe-end and to check for similar problems in the other seven safe-ends. The visual portion of the through-wall crack in the N2A safe-end appeared to be located along the fusion line of the weld repair. The geometry of the crack through the safe-end wall could not be determined at that point in time. However, it was thought that the crack probably initiated in the crevice at the mateing surface at the thermal sleeve in the inside of the safe-end. Examinations at that time revealed linear indications in four other safe-ends. One other safe-end showed some non-linear indications and the remaining two safe-ends had no indications in initial examinations. Representatives of the NRC Region III Office of Inspection and Enforcement reviewed these preliminary NDE results. A summary of those preliminary findings was presented to the NRC at a meeting in Bethesda on June 27, 1978. Further details and preliminary plans for the replacement program were presented to the NRC at a meeting on July 7, 1978.

Subsequent examinations of all safe-ends revealed that all eight safe-ends were cracked. The results of the most recent examinations are included as Table II. B-1.

TABLE II. B-1

Safe-End Designation	UT Results (September, 1978)
A*	Approximately 90° through-wall crack with additional indications for an additional 180° of the ID.
B	Linear 360° indication on the ID in both axial directions which was interpreted as a crack.
C	Same as B
D	Same as B
E*	Intermittent travelling indication for 360° of the ID.
F	Same as B
G	Same as B
H	Same as B

Safe-End Designation	RT Results
A	Crack indication for approximately 270° of ID including through-wall crack for approximately 90°.
B	Crack indication on ID for 360°.
C	Crack indication for approximately 270° of ID with an added approximately 5° indication in middle of remaining 90°.
D	Crack indication for approximately 320° of ID with no indications occurring at two locations for approximately 20° in each location.
E	Crack indication for approximately 160° of ID with intermittent slag indications throughout the thermal sleeve weld.
F	Crack indication on ID for 360°.
G	Crack indication on ID for approximately 260°.
H	Clear crack indications at two locations on the ID for a total of approximately 120°. Intermittent indications on ID for an additional approximate 30°.

*June, 1978 UT Inspection. Both nozzles subsequently sent to SwRI and Battelle.

II.C SAFE END REMOVAL

The effort of removing the safe end-thermal sleeve pieces at DAEC consisted of many activities relative to radiation protection, procedures, shielding design, dimensional control of the cutting operations, protection of the safe end-thermal sleeve samples and preservation of pre-cut piping positions. One of the main pre-cut activities was to ensure the piping systems did not move when the cutting operation was in progress. As the design change package included specifications to restrict piping movements to within 0.010 inches after the cutting was completed, a comprehensive restraint and motion detection system was designed. The system consisted of pipe clamp jacks that restrained the ring header and riser pipes in their position prior to initiating the cutting operations. Motion detection was accomplished by using Linear Voltage Differential Transducers (LVDT's) mounted on the riser pipe elbows. Other activities included: 1) extensive personnel training to ensure minimum radiation exposure; 2) the use of mockups to demonstrate all cutting operations to ensure engineering considerations could be verified and personnel training was adequate; 3) installation of instrumentation to monitor and record all pipe and nozzle movements and strains; 4) extensive quality controls to monitor and audit receiving inspection, mockup training, procedure development, work activities.

Strain gauges were mounted on the recirculation inlet nozzles to monitor bending loads on the recirculation inlet safe ends. This data was utilized to determine the need for axial adjustment of the thermal sleeves to compensate for bending of the internal riser pipes.

The cracked safe end was removed by cutting the safe end and thermal sleeve at a point approximately 2 inches inboard of the crack. A second cut was made near the elbow in the recirculation line allowing the safe end with its attached stainless steel transition piece and attached section or recirculation line to be removed as a unit. This provides access for the repairs and

minimizes the number of cutting operations required to be performed in the radiation area. The transition piece and section of recirculation line were cut from the cracked safe end (approximately 2 inches from the crack) to be reinstalled later along with the replacement safe end. This avoided the need for any bimetallic welds during the repair process.

Upon completion of the first cut through the safe ends, low strains on the order of from 100-150 micro-inches per inch were measured. This indicated that the assembly loads of the thermal sleeves on the safe ends are small and no axial adjustment of the thermal sleeves were necessary.

II.D Cause of Failure

Conclusions regarding the cause of failure are included in the SwRI Interim Report submitted to the NRC on October 27, 1978, and in Section III-B-2 (General Electric Evaluations of Cause of Cracking) of this report.

The cause of cracking of the recirculation inlet riser safe-ends has been evaluated and identified as intergranular stress corrosion cracking (IGSCC). No conclusions regarding the contribution or source of sulphur contamination to the cracking phenomena can be made at the present time.

II.E Status of Remaining Six Safe-ends

The remaining safe-ends are presently stored at the DAEC for possible future evaluations or testing. Iowa Electric will consult with and obtain concurrence of the NRC Staff prior to conducting any destructive testing of these safe-ends.

II.F Replacement Design

A description of the replacement safe-end design is provided in Section III-C-1 of this report. This design was discussed during the July 7, 1978 and November 14, 1978 meetings with the NRC staff and was also described in our July 31, 1978 Repair Report.

II.G Replacement Installation

A description of the replacement safe-end installation is provided in Section III-D of this report.

II.H RESTART PROGRAM

At the completion of the welding effort and acceptance of the NDE results the restart program will be implemented. This program is designed to ensure the plant is restored to the condition prior to the shutdown in June 1978.

The basic program involves reassembling the reactor components, check out of all plant systems, surveillance testing as required by the Technical Specifications, performing the prestart master checklist, startup testing required by the Technical Specifications and the hydrostatic test of the repaired safe ends.

As an example of the program's extensive coverage, every system in the plant will be checked for valve position and instrument operability. This comprises 73 systems. The line-up will be very similar to the initial plant startup in 1974. In order to ensure the operability of instrumentation, pumps and valves in the entire plant, a comprehensive surveillance program has been established to demonstrate the operability of each component. The surveillance program is as follows:

Prior to fuel loading, each department will do the following:

Operations - 9 tests

Electrical Maintenance - 17 tests

After fueld loading and prior to generating electricity each department will do the following:

Operations - 15 tests

Electrical Maintenance - 57 tests

Reactor Engineering - 2 tests

Chemistry - 18 tests

Mechanical Maintenance - 4 tests

II.I Stress Report

A copy of the stress report for the replacement safe-ends is included with this submittal.

III.A.1 History of Unidentified Leakage

During the last 3 years the plant has experienced various shutdowns either due to drywell unidentified leakage increases or unrelated causes. Upon shutdown, the drywell was entered to repair valves and packing in order to decrease the leakage level. The major events of the past 3 years are described below:

During 1975 there were 3 shutdowns due to unacceptable unidentified drywell leakage. Shutdowns were initiated when the leakage reached approximately 3.2, 4.2 and 4.6 gpm. The leakage was due to testable check valve and drywell cooling valve packing leakage.

During 1976 there was no shutdown due to unidentified leakage. However, during the year there were 3 outages for unrelated causes, at which time the drywell was entered to reduce the existing unidentified leakage rate.

During 1977 there was 1 shutdown due to an unacceptable unidentified drywell leakage. The leakage increased to approximately 4.3 gpm due to a feedwater check valve leak. There were 2 shutdowns for hydraulic snubber inspections in the drywell, at which time the existing unidentified leakage rate was reduced by adjusting and replacing valve packings.

In reviewing the past history of drywell unidentified leakage, the Technical Specification limit of 5 gpm has proven

to be an acceptable level for plant operational flexibility and has been determined by General Electric to be an acceptable limit to be applied to inconel material relative to the "leak before break" criteria of stainless steel. If the limit is reduced to a lower value, the flexibility of scheduling plant shutdowns would be reduced and would cause additional thermal cycling of plant systems. If the Technical Specifications had required a shutdown at 2 gpm, the past data show an additional four (4) shutdowns would have been required in the 1975-1977 period. These additional shutdowns were avoided by modifying plant operations to hold the leakage at approximately 2 gpm thus allowing continued operation until an unplanned shutdown occurred. The drywell unidentified leakage source was repaired during the unplanned outages.

III.A.2 Adequacy of Present Technical Specifications

The DAEC technical specification requires that "any time irradiated fuel is in the reactor vessel and reactor coolant temperature is above 212°F, reactor coolant leakage into the primary containment from unidentified sources shall not exceed 5 gpm." This specification is consistent with NUREG-0123, "Standard Technical Specification for General Electric Boilding Water Reactors."

This 5 gpm allowable leakage rate of coolant from the reactor coolant system is based on predicted and observed behavior of cracks in pipes. The detection capability for determining coolant system leakage is also considered in establishing this 5 gpm limit. As discussed in the previous section, the operation history of DAEC clearly indicates that the floor drain sump flow measuring system is sufficient to provide leakage ratio determination at and below the 5 gpm level.

The behavior of cracks in piping systems has been experimentally and analytically investigated almost continuously beginning with the USAEC Sponsored Reactor Primary Coolant System Rupture Study (the Pipe Rupture Study), initiated in 1965. Work in this area is most recently documented by General Electric in NEDO-21000, Investigation of Causes of Cracking in Austenitic Stainless Steel Piping, July 1975.

This work indicates that nuclear piping systems can tolerate cracks, including easily detectable through-wall cracks.

For leakage of the order of 5 gpm, field experience and analytical data demonstrate that an adequate margin of safety exists before a crack approaches the critical size.

The DAEC leak detection system provides diverse methods for determining if an increased leak rate exists within the drywell. In addition to the drywell floor drain sump system mentioned above, the drywell atmosphere radioactivity detector provides a sensitive and rapid indication of increased nuclear system leakage. The drywell containment is continuously sampled from three locations which are chosen to provide both a representative gas mixture and an indication of the leakage location. The sampled air undergoes three separate processes in which the radioactive noble gas, halogen, and particulate contents are determined. The readings for each channel are fed into a pen recorder so that a permanent record of the drywell atmosphere radioactivity is maintained. The particulate detector is the primary indication of leakage, with the halogen and noble gas detectors serving as backup indications of the drywell environment.

Since the background contamination and deposition (chemical reaction effects) cannot be predetermined, and since it is an increase in detected values which indicates a leak,

the alarm points are determined by operator experience. This system serves as an early alarm system to signal the operator that closer examination is necessary to determine the extent of any required corrective action. It therefore provides a diverse leak detection method. The combination of floor drain sump monitoring and the drywell atmosphere radioactivity detection systems meet the intent of Regulatory Guide 1.45 with respect to acceptable detection methods.

III.A.3 Leak Before Break

Although the design basis for nuclear plants includes a postulated pipe break (LOCA), piping and safe-end systems are analyzed, materials are selected, and leak detection systems designed to assure that if a pipe or safe-end should crack, that crack would grow to a leak and the leak would be detected before a crack reaches critical size. This concept has been called leak before break.

In general terms, the leak before break (LBB) concept is built on the fact that reactor piping and safe-ends are fabricated from ductile materials which can tolerate large through-wall cracks without fracture under service type loads. This has been shown by fracture mechanics theory, supported by laboratory tests, full scale tests, and field experience. Further, it has been shown that through-wall cracks which leak at the rate of 5 gpm or less have significant margin before pipe rupture.

The bases for leak before break for axial flaws has been presented in GESSAR (Ref. III.A.3-1). These bases were subsequently expanded in the case of circumferential flaws and documented in NEDO-21000 (Ref. III.A.3-2). In the following sections, the technical bases for circumferential flaw evaluation has been updated to reflect recent test

data and analytical development for predicting critical flaw dimensions. Although the following analyses were originally developed for stainless steel piping, because of similar mechanical properties and geometries the same conclusions can be drawn for Alloy 600 safe-end applications. See III.B-2.

Circumferential Crack Assessment

Recent work by General Electric has led to better modeling of circumferential critical crack phenomena than is reported in NEDO-21000 (Reference III.A.3-2). This modeling uses the Net Section Collapse Criterion (Reference III.A.3-3).

For materials exhibiting highly ductile behavior, such as BWR piping or safe-ends, failure criteria based on brittle fracture or linear elastic fracture mechanics considerations are not valid since failure is characterized by gross yielding and subsequent plastic instability. In the following analysis it is assumed that a pipe with a circumferential crack is at the point of incipient failure when the net section at the crack forms a plastic hinge and the pipe is ready to collapse. The net section collapse criterion is simple to apply and has been shown to be effective in

predicting failure of cracked ductile components by Electric Power Research Institute Report NP-192 (Reference III.A.3-4), and the NRC (Reference III.A.3-5).

In order to determine the point at which collapse occurs, for a circumferential crack of length, l, and depth, d, located on the inside section of the pipe (Figure III.A.3-1), it is necessary to apply the equation of equilibrium assuming that the cracked section behaves like a hinge. For this condition the stress state at the cracked section is as shown in Figure III.A.3-1 where the maximum stress is the flow stress of the material o_f. Further, the flow stress has been shown to be a function of the ultimate strength of material o_u and the yield strength o_y and can be approximated by $(o_u+o_y)/2$. The angle, B, at which stress inversion occurs can be determined for equilibrium in the longitudinal direction. If P_m is the primary membrane stress in the longitudinal direction in the uncracked section of the pipe, it can be shown that B is given by:

$$B = \frac{o_f(ll - a\frac{d}{t}) - P_m ll}{2o_f} \qquad \text{(Equation I)}$$

The maximum primary bending stress, P_b, is determined by equating the moments in the crack section to the applied moments in the uncracked sections of the pipe when the flaw parameters are critical. In this case:

$$P_b = \frac{2o_f}{ll} \; 2 \sin B - \frac{d}{t} \sin a \qquad \text{(Equation 2)}$$

Equations (1) and (2) together define the combinations of a and d/t for which failure by collapse will occur under the given applied stresses P_m and P_b.

For normal steady state conditions of operation, the only primary stress of significance is the PR/2t pressure stress. The bending stress due to dead weight is small and can be ignored.

By solving equations (1) and (2) for a through-wall crack with d/t = 1.0 it is demonstrated that a through-wall crack of up to 55% of the circumference can be tolerated with o_f = 50 Ksi and P_m = 5.4 Ksi. In other words, the critical crack length is 55% of the pipe circumference. For schedule 80 4" and 12" pipes we therefore obtain the following:

Nominal Pipe Size (Schd 80), in.	Avg Wall Thick, in.	Circumferential Critical Crack Length, in.
4	0.337	6.9
12	0.687	20.7

The results are comparable to the axial critical crack length calculations. Either axial or circumferential critical crack lengths can therefore be compared to limiting crack length for 5 gpm leakage flow to assess safety margins for the leak detection system.

Leakage Flow Rate for Circumferential Cracks

The maximum flow rate for blowdown of saturated water at 1000 psi is 55 lb/sec-in^2. Friction in the flow passages reduces this rate but can be ignored in piping geometries for leakages. The required crack size for 5 gpm saturated water flow, under these conditions, is

$$A = 0.0126 \text{ in.}^2$$

Given this area, and determining the crack opening displacement, w, the crack length 1 for a 5gpm leakage rate can be determined.

For circumferential cracks, the crack opening displacement has been treated in NEDO-21000 and is similar to GESSAR except that the applied nominal stress is now equal to PR/2t, giving a longer crack length to yield a 5 gpm leak rate. In NEDO-21000, the comparison for the same 4" and 12" pipe sizes gives:

Nominal Pipe Size (Sch 80), in.	Avg Wall Thick, in.	5 gpm Crack Length, in.	Ratio (5gpm)/(critical)
4	0.337	5.9	0.86
12	0.687	7.4	0.35

This comparison shows that even for the lower operating stress on the circumferential crack opening, substantial margin exists from the 5 gpm leakage crack length to the critical crack length.

It is important to recognize that the failure of ductile piping with a long through wall crack is characterized by large crack opening displacements which precede unstable rupture. Judging from observed crack behavior in the GE and BMI experimental programs involving both circumferential and axial cracks, it is estimated that leak rates at hundreds of gpm will precede crack instability. Measured crack opening displacements for the BMI experiments were in the range of 0.1 to 0.2 in. at the time of incipient rupture, corresponding to leaks of the order of 1 sq. in. in size.

Experience at DAEC

The recirculation inlet safe-end crack at DAEC consisted of a through wall crack over approximately 80 degrees of the 360 degree circumference. This crack leaked at about 3.2 gpm which is less than would be expected for circumferential cracks of this length. Because of the crevice geometry and the fact that the safe-end is thicker than schedule 80 pipe at the crack location, friction along

the wetted crack length could have contributed to a reduction in the leakage. Also, the moderate leak rate observed suggests that the crack opening displacement was small, which in turn suggests that the crack was not close to critical size. It should be noted that the crevice geometry and the associated restricted path leakage have been removed from the pressure boundary in the replacement configuration.

REFERENCES

Section III.A.3

1. GESSAR, General Electric Standard Safety Analysis Report, 238 Nuclear Island, Docket STN 50-447, Section 5.2.7.

2. H. H. Klepfer, et. al., "Investigation of Cause of Cracking in Austenitic Stainless Steel Piping," NEDO-21000, July 1975.

3. S. Ranganath, "Failure Analysis Diagram for Circumferential Cracks in Austenitic Piping", May 26, 1978. GE letter RSFA-78-01.

4. "Mechanical Fracture Predictions for Sensitized Stainless Steel Piping with Circumferential Cracks", EPRI Report NP-192, Final Report September 1976.

5. "Review and Assessment of Research Relevant to Design Aspects of Nuclear Power Plant Piping Systems", NUREG-0307, Nuclear Regulatory Commission, July 1977.

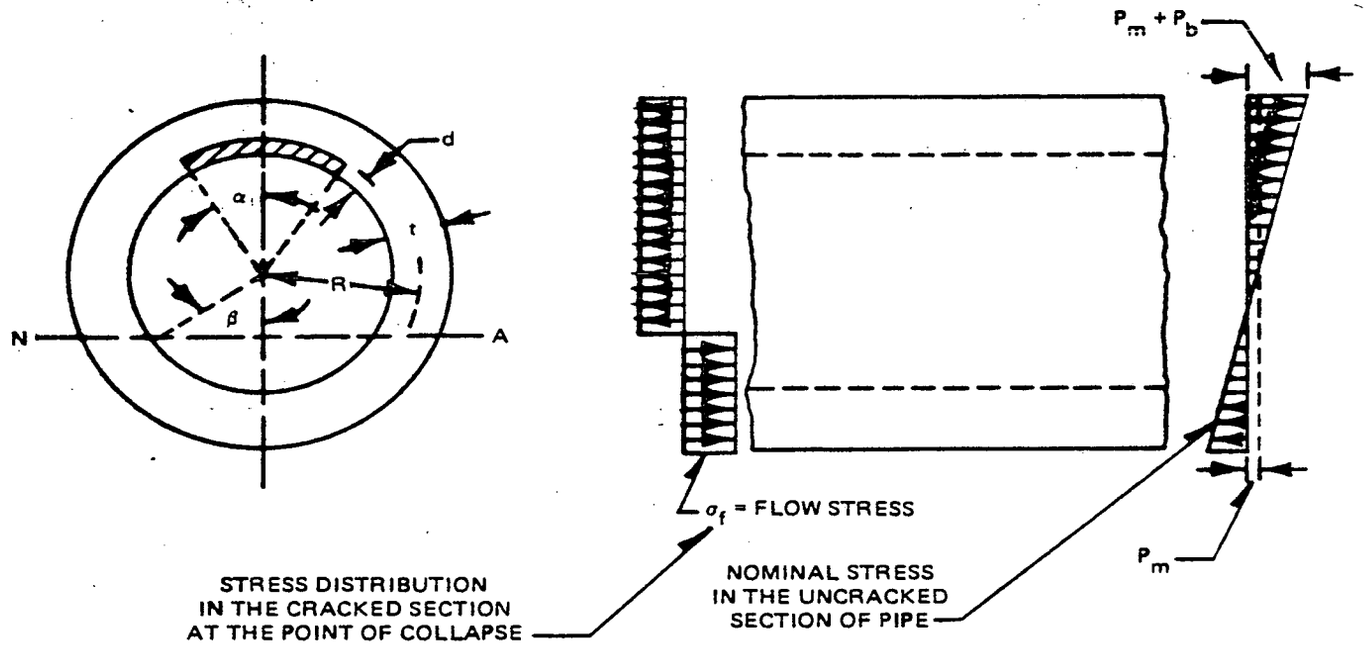

Figure III.A.3-1. Schematic Showing Stress Distribution in a Cracked Pipe at the Point of Collapse

III.A.4 Modifications To Existing Equipment

IE is presently considering modifications to the DAEC drywell leak detection capabilities.

The first modification under consideration would be to modify the floor drain sump fill timer sensitivity to detect a 1 gpm increase in one hour above a 1 gpm baseline leakage rate. This would require modifications in the sump system circuity.

A second modification would be to have an analog signal from the sump level transmitter for the entire range of the sump level sent to the DAEC process computer. The computer can calculate the rate of change of the sump level every minute and have it printed out on an alarm typer and the B.O.P. log each hour. Of course, the alarm in the control room could be set for any desired rate of change in leakage.

The third modification being considered would be a study to model and correlate drywell iodine levels with unidentified leakage. From this a computer model could develop to predict unidentified leakage from the iodine level in the drywell atmosphere.

III.B.1 SwRI REPORT

The final SwRI report "Metallurgical Investigation of Cracking in a Reactor Vessel Safe End" will be submitted to the NRC by December 22, 1978. There are no anticipated significant deviations from the conclusions presented in the interim report submitted to the NRC by letter dated October 27, 1978.

The final report will address the extent of the lack of fusion in the safe end to thermal sleeve weld which was briefly discussed in the November 14, 1978 meeting.

In addition to the above, the report will include a literature review concerning stress corrosion cracking susceptibility of Alloy 600 as referenced in the October 27, 1978 letter.

SwRI is proceeding with an analysis of the sulfur deposits found on the fracture surfaces near the crack tip. The results of this analysis are necessary to determine the source of the sulfur.

III.B.2 GENERAL ELECTRIC EVALUATION OF CAUSE OF CRACKING

Based on the photo micrographs of the DAEC safe ends reported by Southwest Research Institute and Battelle Memorial Institute, GE concludes that the cracking was due to Intergranular Stress Corrosion Cracking (IGSCC).

It has long been established that stress corrosion cracking (SCC) occurs as the result of the interaction of a susceptible material, an appropriate environment and a tensile stress above a threshold value. The control or elimination of any one of these three major variables (material, environment, tensile stress) is sufficient to eliminate SCC.

A material may be susceptible to SCC due to its alloy composition, a heat treatment such as sensitization, cold work or surface preparation. An appropriate environment may consist of a specific corrosive medium, or a non-corrosive medium becoming corrosive as a result of (1) high temperature, (2) contamination such as excess chloride, flouride, sulphate or oxygen, (3) a concentrating mechanism such as alternate wetting and drying or (4) a crevice. The tensile stresses may be a combination of applied primary, secondary, or residual stress. The residual stresses may be present due to previous plastic deformation or welding.

The DAEC Alloy 600 safe end material would have become more susceptible to cracking due to a re-solution of the carbide phase by welding and the subsequent grain boundary precipitation of chromium rich carbides ($M_{23}C_6$) which tends to leave the adjacent material chromium depleted. The environment became more aggressive due to the presence of a crevice with its concomitant chemistry at the safe end to thermal sleeve joint. These two factors combined with the presence of high (over yield) total applied tensile stress due to primary plus secondary (including residual stresses) stresses produced IGSCC. The contributing factors for this phenomena are summarized in Figure III.B.2-1.

In order to further understand the nature of this localized form of stress corrosion cracking, it is best to examine first the significantly large IGSCC data base for furnace sensitized Type 304 austenitic stainless steel which is susceptible to IGSCC in high temperature oxygenated water as a result of the same chromium depletion mechanism. Figure III.B.2-2 presents a correlation of the results of numerous stress corrosion tests in a simulated and actual BWR reactor water at 550°F using small uncreviced laboratory type specimens such as uniaxial tension, biaxial tension (pressurized tubes) and bent beams (Reference III.B.2-1). The figure plots the time to cracking versus the applied stress. The lower the applied tensile stress, the greater the time necessary to produce IGSCC. As the applied stresses are reduced to the yield stress of the material, the median cracking time rapidly increases to the point where no cracking is identified even after extremely long hold times. This asymptotic relationship is typical of stress corrosion phenomena in numerous environments as demonstrated by some recent studies by Vignes and Combrade, (Reference III.B.2-2), where the failure threshold stress was identified as the 0.2% offset yield stress on Alloy 600 constant strain specimens in 10% NaOH deaerated solutions at 320°C.

Figure III.B.2-3 presents the previous plot of furnace sensitized Type 304 stainless steel superimposed on a similar plot of the relationship between applied stress and median time to cracking for uncreviced Alloy 600 as taken from the data of numerous investigators, (References III.B.2-3, III.B.2-4, III.B.2-5, III.B.2-6). It is important to note some subtle differences between Figures III.B.2-2 and III.B.2-3. First of all, the median cracking time is expressed in years in Figure III.B.2-3 as opposed to hours in Figure III.B.2-2, resulting in a shift in the position of the stainless steel curve of approximately four decades to the left. Secondly, since the yield strength of the two materials are different, 40 $\pm$ 13 KSI and 23 $\pm$ KSI at 550°F, for Alloy 600 and Type 304, respectively, it would be meaningless to compare the two materials as a function of applied stress. Therefore, the two materials are normalized by plotting the median time to failure as a function of an applied stress ratio. The third factor that should be noted is that many of the data points used to plot the general

shape of the Alloy 600 curve were obtained from laboratory studies at slightly higher temperatures (572°F) than typical of the BWR (545°F). Since high temperature is an accelerant to IGSCC, this curve is somewhat conservative. Finally, the curve drawn for the Alloy 600 samples is an estimate of the laboratory results since none of the samples shown have failed.

A comparison of the two curves indicates that uncreviced Alloy 600 is more resistant to IGSCC than furnace sensitized uncreviced Type 304. In fact, no uncreviced Alloy 600 cracked in simulated BWR environment. However, when Alloy 600 becomes creviced through the use of test specimen configurations such as double U-bends, double tensiles, banded tensiles or surface pickling, the Alloy 600 does suffer from IGSCC as shown in Figure III.B.2-4.

All available data indicates that over yield stresses are required to initiate IGSCC in Alloy 600 in the BWR environment. This is consistent with and analogous to the behavior of welded Type 304 stainless steel. Based on this threshold stress dependency, the use of the stress rule criteria employed successfully for Type 304 stainless steel is equally applicable to Alloy 600 and is described as follows:

Since a high total combined stress is a required contributing factor to IGSCC, it can be prevented by limiting the stress on a component or pipe even in the sensitized condition. This is why most pipes (and furnace sensitized components) have not cracked. Field cracks, which have been observed to occur in the same locations at several plants, demonstrate that over yield stress level is indeed a necessary factor in intergranular stress corrosion cracking as summarized in Figures III.B.2-3 and III.B.2-4.

It is important when evaluating IGSCC margin to include all forms of stress. Primary (pressure + weight) stresses are the most significant stresses as shown by environmental tests. Secondary (thermal) stresses, peak (local) stresses, and residual stresses also contribute and must be included in any evaluation of stresses contributing to intergranular stress corrosion cracking.

Formulation of stress rules to evaluate components and pipes has been based on laboratory and field data. General Electric Laboratory tests on Type 304 stainless steel indicate that the sustained stress and strain state of a material must exceed its 0.2% offset yield stress for intergranular stress corrosion cracking to become a potential problem, Figure III.B.2-2. Thus, if the stresses of a component are below the flow curve of the material, intergranular stress corrosion cracking will not occur.

The following stress rule (Figure III.B.2-5) is formulated to assure that this condition is met:

$$\frac{P_m + P_b}{S_y} + \frac{Q+F+[RESID]}{S_y + .002E} \leq 1$$

P_m = primary membrane stress

P_b = primary bending stress

S_y = ASME code 0.2% offset yield stress at applicable temperature

Q = secondary stress

$[RESID]$ = Residual Stress (defined below)

F = peak stress

E = elastic modulus of the material at service temperature

The term $[RESID]$ which accounts for residual stresses is defined as follows: Within 1 inch of a weld $[RESID]$ shall be assumed to be equal to the appropriate value from Figure III.B.2-6. These values are based on the envelope of maximum axial values measured on Schedule 80 stainless steel pipe sizes of the range 4" - 26". The values for Alloy 600 were obtained by multiplying the stainless steel values by the 550^{o}F yield stress ratio of stainless steel to Alloy 600.

The stress rules outlined above have been used by General Electric in selected cases to identify those piping welds which may be susceptible to intergranular stress corrosion cracking.

A summary of the BWR field experience for which stress rule evaluations have been performed is contained in Figure III.B.2-7. Detailed stress information is available on a total of 93 Type 304 weld cracking incidents; none of these 93 incidents occurred at stress index values below 1.2.

The only known BWR field cracking incidents of Alloy 600 components are the DAEC recirculation inlet safe ends. The stress rule index for the specific location where IGSCC was observed (the root of the crevice formed by the attachment weld between the thermal sleeve and safe end) was calculated and found to be 2.24 as indicated in Figure III.B.2-8. As indicated, the residual stress component of the stress rule index is 0.46. This component contributes approximately 20% to the total stress rule index value. Although this contribution is significant, GE concludes that the residual stress is not the principal driving force for the cracking since the uniform stresses other than residual stresses contribute approximately 50% of the total stress rule index value.

In one other similar but lower stressed Alloy 600 application at an overseas GE BWR a detailed inservice examination was made. In 1976, General Electric Company and its licensee were able to examine the two feedwater nozzles of an overseas BWR plant. The feedwater nozzles in this plant are entirely made from Alloy 600 forgings. The thermal sleeve to nozzle weld is of a fillet weld configuration with a very tight crevice formed between the two components. After ten years of operation no evidence of cracking was found in the creviced Alloy 600 nozzles by visual, dye penetrant, ultrasonic or radiographic examination. Although no detailed stress report is available for this location, an evaluation recently performed by General Electric indicated that the stresses were likely to be moderately high in this area; with a stress rule index value of approximately 1.2. This is significantly lower than the 2.24 stress index value calculated for the DAEC case.

In addition the failure time of the DAEC safe end can be compared with the laboratory data for creviced Alloy 600. While the technical difficulties in making such a comparison between data obtained on small laboratory samples and a full size component are significant, this information may provide some useful insight in evaluating other creviced applications including the replacement design. Such an analysis requires the estimation of the IGSCC crack propagation rate following crack initiation.

The stress analysis of the DAEC safe end reveals a stress rule index value of 2.24 and the safe end began leaking after 3.3 years of operating exposure. If stress index is used as a stress ratio, this point, with 3.3 years exposure, would fall far to the right of the creviced Alloy 600 data. By assuming that the small specimen data adjacent to the crevice curve represents the initiation time, then a resulting propagation rate could be hypothesized.

Although applied stress ratio and stress rule index are not directly equivalent in all cases, the stress rule index can be used as an approximate value for obtaining a time to failure point from Figure III.B.2-4.

From Figure III.B.2-4 it can be estimated that crack initiation begins in 0.2 years or less at an applied stress ratio of 2.24. Since a leaking crack of about 0.7 inch depth occurred in 3.3 years, the average estimated propagation rate is on the order of

$$\frac{0.7}{3.3 - 0.2} = .226 \text{ inches/year}$$

or 0.6 mils/day

This value is less than the upper bound for 304 stainless steel field cracking rates of 1-10 mils/day (Reference III.B.2-1). The actual instantaneous propagation rate is dependent on the stress intensity at the propagating crack tip and this intensity varies with crack depth in a complex manner because of the variation of residual, peak and bending stresses through the safe end wall.

A critical aspect of Figure III.B.2-4 is why the creviced material suffers from IGSCC while the uncreviced Alloy 600 has a high resistance to IGSCC in similar bulk environments. The phenomenon of crevice corrosion is characterized by a geometrical configuration in which the cathodic reactant (usually dissolved oxygen) can readily gain access by convection (forced and natural) and diffusion to the metal surface outside the crevice, whereas access to the layer of the stagnant solution within the crevice is far more difficult and can be achieved by diffusion or capillary action through the mouth of the crevice. This results in a difference in concentration of the cathode reactant at the two surfaces.

Metals and alloys that rely on passivity (e.g., the formation of a protective film) for their corrosion resistance can be prone to crevice corrosion attack. The environment can be any aggressive solution (acid or neutral), such as high temperature - high purity water with dissolved oxygen. It should be noted that solutions containing excess amounts of chloride or sulfate ions are highly conducive to crevice corrosion. The crevice must be wide enough to allow entry of the solution, but sufficiently narrow to maintain a stagnant zone of solution within the crevice so that entry of the cathode reactant and removal of their reaction products is extremely slow and occurs only by diffusion and migration (if the species is charged). If a crevice can be flushed regularly, then a special concern for crevice accelerated corrosion is not warranted.

The mechanism responsible for the decrease in time to cracking or in fact the cause of cracking itself for creviced Alloy 600 in BWR type environments is illustrated in Figure III.B.2-9. The crevice represented in Figure III.B.2-9 could be, for example, the narrow space between double U-bend specimens, double tensile specimens or a mechanical seal or joint such as the DAEC welded safe end to thermal sleeve joint. Since no ionic specie of nickel, the main alloy element of Alloy 600, is stable in neutral water at BWR operating temperatures ($\sim 300^{\circ}C$), then the following interim reaction will occur:

$$Ni \rightarrow Ni^{++} + 2e^{-} \quad \text{(oxidation)}$$

The reduction reaction accompanying the above oxidation reaction is the cathodic reduction of the dissolved oxygen:

$$O_2 + 2H_2 + 4e^- \rightarrow 4OH^- \quad \text{(reduction)}$$

Initially, these two reactions occur uniformly over the entire surface, including the interior of the crevice. Charge conservation is maintained in both the metal and solution. Every pair of electrons produced during the formation of a nickel (or other alloying element) ion are immediately consumed by the oxygen reduction reaction. Two hydroxyl ions are also produced for every divalent cation in the solution. After a short interval, the 0.2 ppm oxygen initially in the crevice is depleted due to the restricted convection and diffusion discussed earlier and therefore oxygen reduction ceases in this area. This, by itself, does not result in any modification of the overall corrosion reaction. Since the area within the crevice is usually relatively small compared to the external area, the overall effect on the rate of oxygen reduction is almost immeasureable. Thus, the rate of corrosion within and without the crevice remains equal.

Therefore, the critical corrosion reaction is not the depletion of oxygen itself, but rather the termination of the oxygen reduction reaction while the dissolution of the metal continues. This tends to produce an excess of unstable positive charge in the solution (Ni^{++}). The Ni^{++} in solution can hydrolyze and precipitate as shown in the following equation:

$$Ni^{++} + 2H_2O \rightarrow Ni(OH)2\downarrow + 2H^+ \quad \text{(hydrolysis)}$$

This, however, still leaves an excess positive charge in solution since two positively charged hydrogen ions have simply replaced the one double positively charged nickel ion. This excess positive charge in the solution is necessarily balanced by the migration of ions into the crevice to maintain neutrality. Negatively charged anions such as chloride, flouride, sulphate and other anions migrate to this negatively charged depleted region. This results in the following possible additional hydrolysis reactions:

$$\left[Ni^{++} + 2Cl^{-}\right] + 2H_2O \rightarrow Ni(OH)_2\downarrow + 2H^{+} + 2Cl^{-}$$

$$\left[Ni^{++} + SO_4^{=}\right] + 2H_2O \rightarrow Ni(OH)_2\downarrow + 2H^{+} + SO_4^{--}$$

The above equations thus indicate an aqueous solution of nickel chloride or sulphate dissociates into an insoluble hydroxide and a free acid. Both chloride and sulphate ions accelerate the dissolution rate of Alloy 600. Since both ions are present in the crevice as a result of migration and hydrolysis then the dissolution rate of nickel is increased. This increase in anodic dissolution produces more $Ni(OH)_2$ which in turn means more positively charged hydrogen ions in solution (decrease in pH) which must be electrically neutralized by the migration of additional negatively charged anions such as chloride and sulphate. Thus, the higher the initial chloride or sulphate content of the solution, the more rapid the reaction kinetics. This has been clearly demonstrated by Pickett (Reference II.D.1-6), Carlen and Blom (Reference III.B.2-9), and Blom and Tyrell (Reference III.B.2-10).

The net result of this increase in acidity (decrease in pH) is a rapidly accelerating process. This rapid dissolution process combined with the presence of a tensile stress (either applied or residual) results in stress corrosion cracking. The crack propagation rate is thus determined by the combined integrated current of all the dissolution transients plus the finite strain rate at the tip of the crack. After a crack is initiated, the crack itself acts as its own crevice. This explains how pickled surfaces can result in premature cracking due to the formation of micro-crevices in grain boundaries and why sensitized and pickled Alloy 600 with 1 to 7 mils of intergranular attack (IGA) cracks in comparable times to that of sensitized unpickled - creviced specimens. (Reference III.B.2-6)

Thus, the above discussion readily explains the difference in SCC performance of Alloy 600 as exposed to simulated BWR environments in the creviced and uncreviced condition. It should be noted that the potential for IGSCC in Alloy 600 increases significantly with increasing temperature. There have been no reported occurrences of Alloy 600 IGSCC in oxygenated pure water at

low temperatures (<200°C). The air saturated conditions (~8 ppm O_2) expected during shutdown/startup conditions, while increasing the oxygen content of the water, would not be expected to significantly impact the stress corrosion response during this period of time since temperature levels are low. Once the temperature of the plant is increased the oxygen level in the water would reduce to that in the normal BWR environment (0.2 ppm O_2).

It has been noted how contaminants such as chloride and sulphate can migrate to creviced regions in order to maintain electro-neutrality and create a free acid environment which increases the dissolution of Alloy 600 and thus increases its sensitivity to IGSCC. However, the presence of sulfur in solution may contribute to the premature IGSCC of creviced Alloy 600 by an additional mechanism.

Coriou, et al (Reference III.B.2-11) have demonstrated that sulfur segregated to grain boundaries in nickel rich alloys may be an extremely detrimental species in terms of electrochemical processes occurring at the grain boundary. Sulfur dissolved in the matrix may increase the active corrosion behavior during a repassivation transient, as identified in stainless steel by Wilde and Armijo (Reference III.B.2-12). After the sulfur-rich grain boundary dissolves, the sulfur would be in aqueous solution, possibly in some deleterious form such as S^-, H_2S or polythionic acid (Reference III.B.2-13) aside from the sulphate mentioned above. These species, coupled with the low pH in the crevice due to the presence of excess hydrogen ions (hydrochloric or sulphuric acid as mentioned above), the thick corrosion film, and the high tensile stresses could account for a premature initiation and subsequent propagation of stress corrosion cracking in the weld heat affected zone of the Alloy 600 safe end by a film rupture repassivation mechanism, i.e., continuous rupture and reformation of the passive corrosion film.

There is additional direct experimental evidence that sulfur containing species in solution can accelerate IGSCC in Alloy 600. Cowan and Gordon cracked a sensitized (24 hours at 1150°F) sample stressed at 50 Ksi in 550°F (Reference III.B.2-16) 100 ppm oxygenated water containing dilute amounts of KSCN (0.5M).

The failure time was 419 hours compared to no failures identified under identical environments without KSCN after over 2500 hours of exposure.

Elemental sulfur was identified by X-ray analysis in the corrosion product at the crack tip of the cracked Alloy 600 safe end by Southwest Research Institute and by Battelle Memorial Institute. It therefore appears that indeed sulfur or sulphate present at the crack location from whatever source may have contributed to the premature cracking of the Alloy 600 safe end.

REFERENCES

SECTION III.B.2

1. H. H. Klepfer, et. al., "Investigation of Cause of Cracking in Austenitic Stainless Steel Piping," NEDO 21000, July 1975.

2. A. Vignes and P. Combrade, "Caustic Stress Corrosion Cracking of Inconel 600 Tubes," paper presented at the 7th International Congress of Metallic Corrosion, Rio de Janiero, October 1978.

3. W. Hubner, M. DePourbaix and G. Ostberg, "Stress Corrosion Cracking of Stainless Steel and Nickel Base-Alloys in Chloride Containing Water and Steam at 200-300°C," Proceedings of the Fourth International Congress on Metallic Corrosion, NACE, Houston, Texas, 1972.

4. Wittubner, B. Johannson (Rosborg) and M. dePourbaix, "Studies of the Tendency of Intergranular Corrosion Cracking of Austenitic FeCrNi Alloys in High Purity Water at 300°C," AE-437, 1971.

5. R. L. Cowan, "Summary of Joint NED-CR&D Corrosion Program for 1970," 1970.

6. A. E. Pickett, "Inconel 600 Review Presentation-Ex-Reactor SCC Test Results," October 6, 1975.

7. R. L. Cowan, "Mechanism of IGSCC of Inconel", GE Report 1971.

8. Inconel Alloy 600, Huntington Alloy Products Division, The International Nickel Company, Inc. Huntington, W. Virginia, May 1969.

9. J. C. Carlen and U. Blom "Influence of Analysis, Heat Treatment and Structure on Susceptibility to Intergranular Stress Corrosion Cracking of Nickel-Chromium-Iron Alloys (Alloy 800 and Alloy 600)", paper presented at the International Nuclear Industries Fair, October 16-21, 1972, Basel, Switzerland Paper #117.

10. U. Blom and M. Tyrell, "Corrosion Resistance of Alloy 600 and Alloy 800 in Chloride containing High-Pressure", paper presented at Corrosion 75, Toronto, Canada, April 14-18, 1975 paper #114.

11. H. Coriou, L. Grall, C. Mahieu and M. Pelas, "Sensitivity to Stress Corrosion and Intergranular Attack of High-Nickel Austenitic Alloys," Corrosion, Vol. 22, 1966.

12. B. Wildle and J. S. Armijo, "Influence of Sulfur on the Corrosion Resistance of Austenitic Stainless Steel," Corrosion, Vol. 23, No. 7, July 1967.

13. J. J. Heller and G. R. Prescott, Materials Protection, vol. 4, 14, 1965.

14. D. A. Vermilyea and M. E. Indig, J. Electrochemical Society, Vol. 119, 39, 1972.

15. D. A. Vermlyea and M. E. Indig, Corrosion and Electrochemical Studies in Aqueous Solutions at 289°C, paper presented 5th International Conference on Metallic Corrosion, Tokyo, 1972.

16. R. L. Cowan and G. M. Gordon, "Intergranular Stress Corrosion Cracking and Grain Boundary Composition of Fe-Ni-Cr Alloys," Stress Corrosion Cracking and Hydrogen Embrittlement of Iron Base Alloys, Conference at Unieux-Firminy, France June 12-16, 1973 Volume published 1977 by NACE, Houston, Texas.

EVALUATION OF DUANE ARNOLD RECIRCULATION INLET

SAFE END CRACKING

- CAUSE - INTERGRANULAR STRESS CORROSION CRACKING
- FACTORS CONTRIBUTING TO CRACK INITIATION

  HIGH TOTAL APPLIED TENSILE STRESSES

  - PRIMARY
  - SECONDARY (INCLUDING RESIDUAL STRESSES)

  CREVICED CONDITION ON PRESSURE BOUNDARY

  SUSCEPTIBLE REGION CAUSED BY RE-SOLUTIONING OF CARBIDE PHASE AND SUBSEQUENT GRAIN BOUNDARY PRECIPITATION (REVEALED BY PHOSPHORIC ACID ETCH).

Figure III.B.2-1

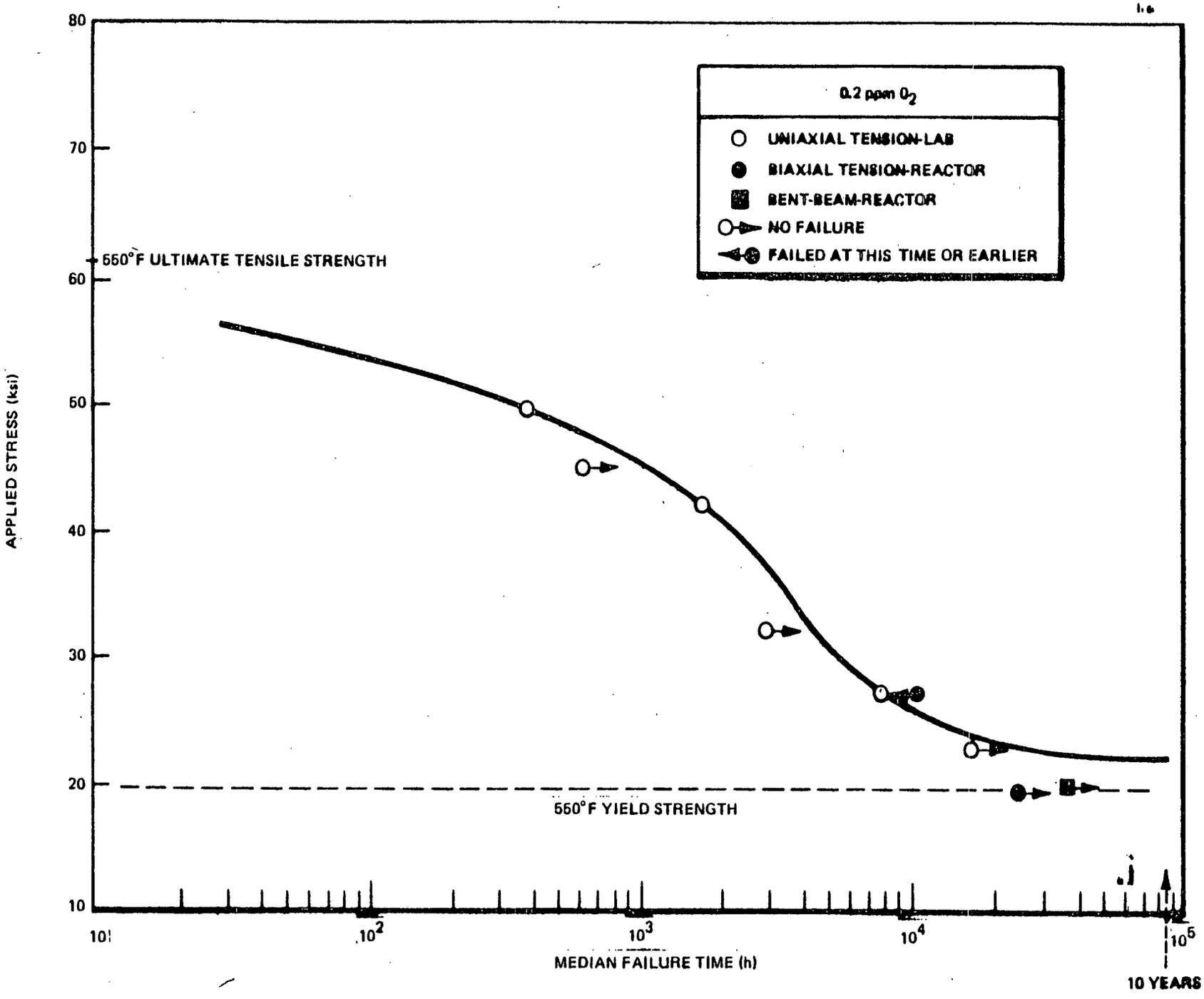

Figure III.B.2-2. Stress Dependency for IGSCC of Furnace-Sensitized Type-304 Stainless Steel in 550°F Water

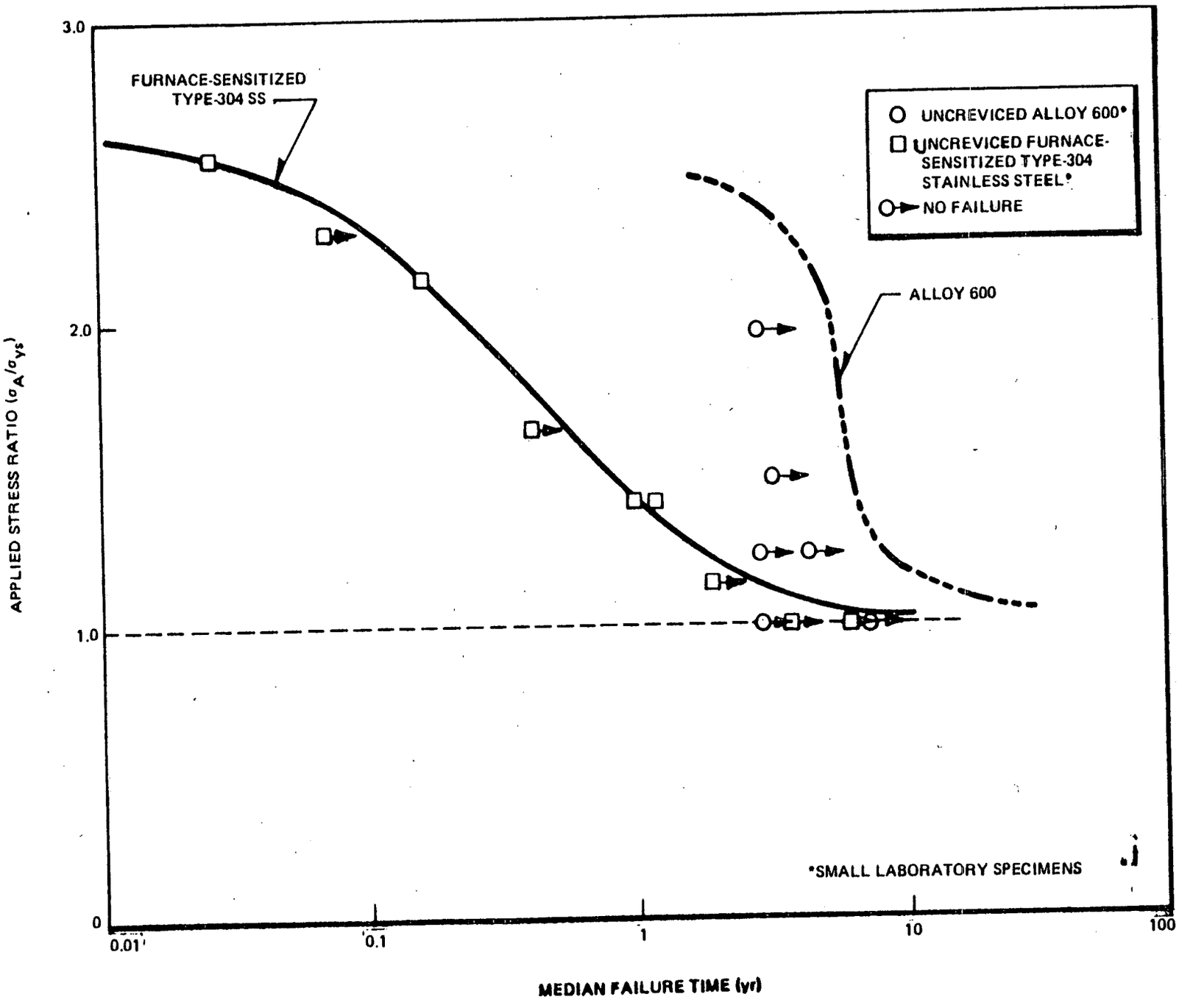

Figure III.B.2-3. Laboratory Results on the Stress Dependency of IGSCC of Alloy 600 and Furnace-Sensitized Type-304 in High Temperature - 0.2 O_2 Water

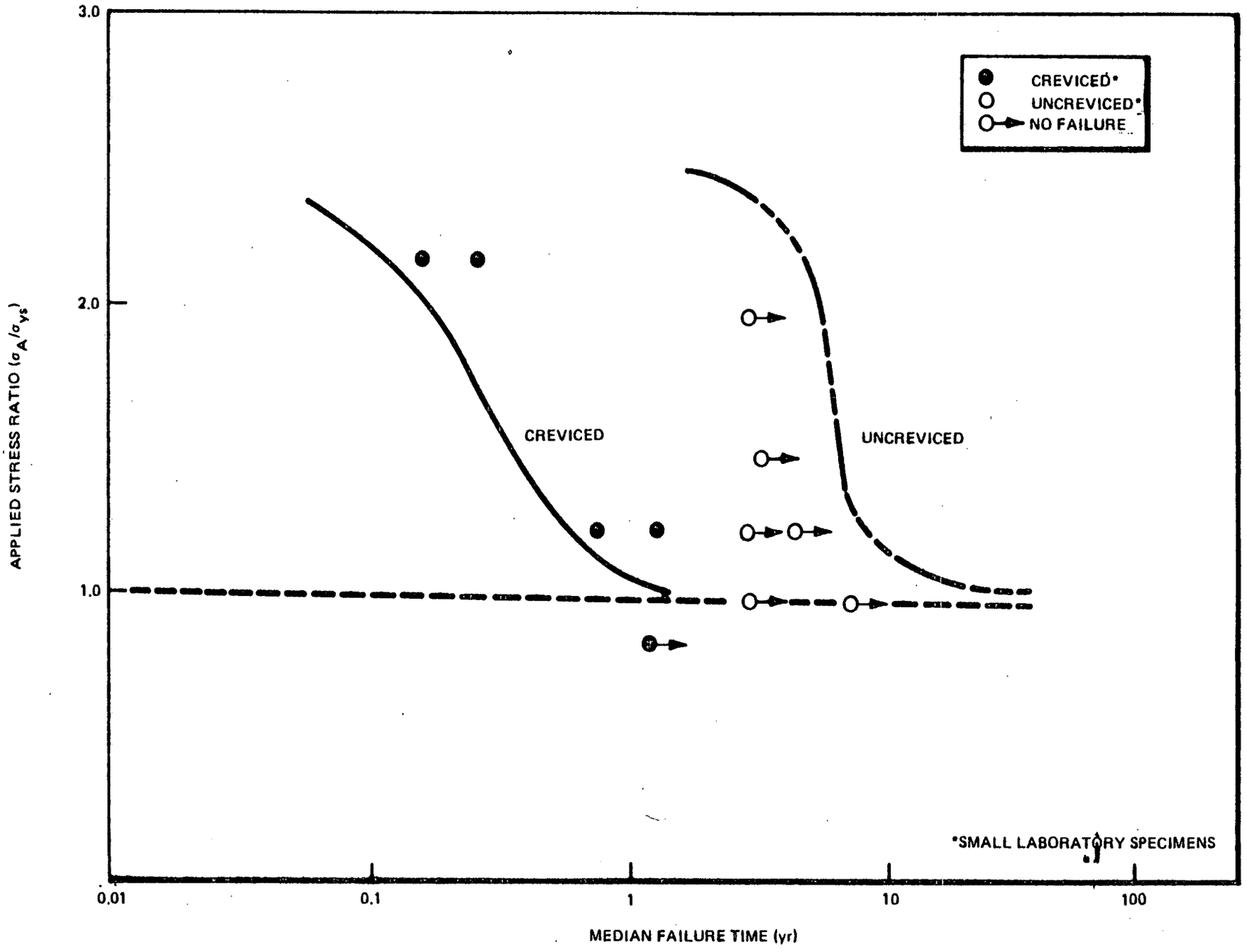

Figure III.B.2-4. Laboratory Results on the Stress Dependency of IGSCC of Alloy 600 in High Temperature - 0.2 O_2 Water

STRESS CORROSION CAN BE AVOIDED IF STRESSES ARE MAINTAINED BELOW 0.2% OFFSET YIELD STRESS

RULE: $$\frac{P_M + P_B}{S_Y} + \frac{Q + F + (\text{RESIDUAL})}{S_Y + 0.002\,E} \leq 1$$

DEFINITIONS:

$P_M + P_B$ = PRIMARY MEMBRANE AND BENDING STRESSES

S_Y = ASME CODE 0.2% YIELD STRESS AT APPLICABLE TEMPERATURE

Q = SECONDARY STRESS (INCLUDES THERMAL)

F = PEAK STRESS

E = ASME CODE ELASTIC MODULUS AT APPLICABLE TEMPERATURE

(RESIDUAL) = SUM OF ALL SOURCES OF RESIDUAL STRESS (INCLUDING WELD RESIDUAL STRESS AND STRESS RESULTING FROM COMPRESSIVE TRANSIENTS)

Figure III.B.2-5. Stress Rule Being Used to Avoid Stress Corrosion

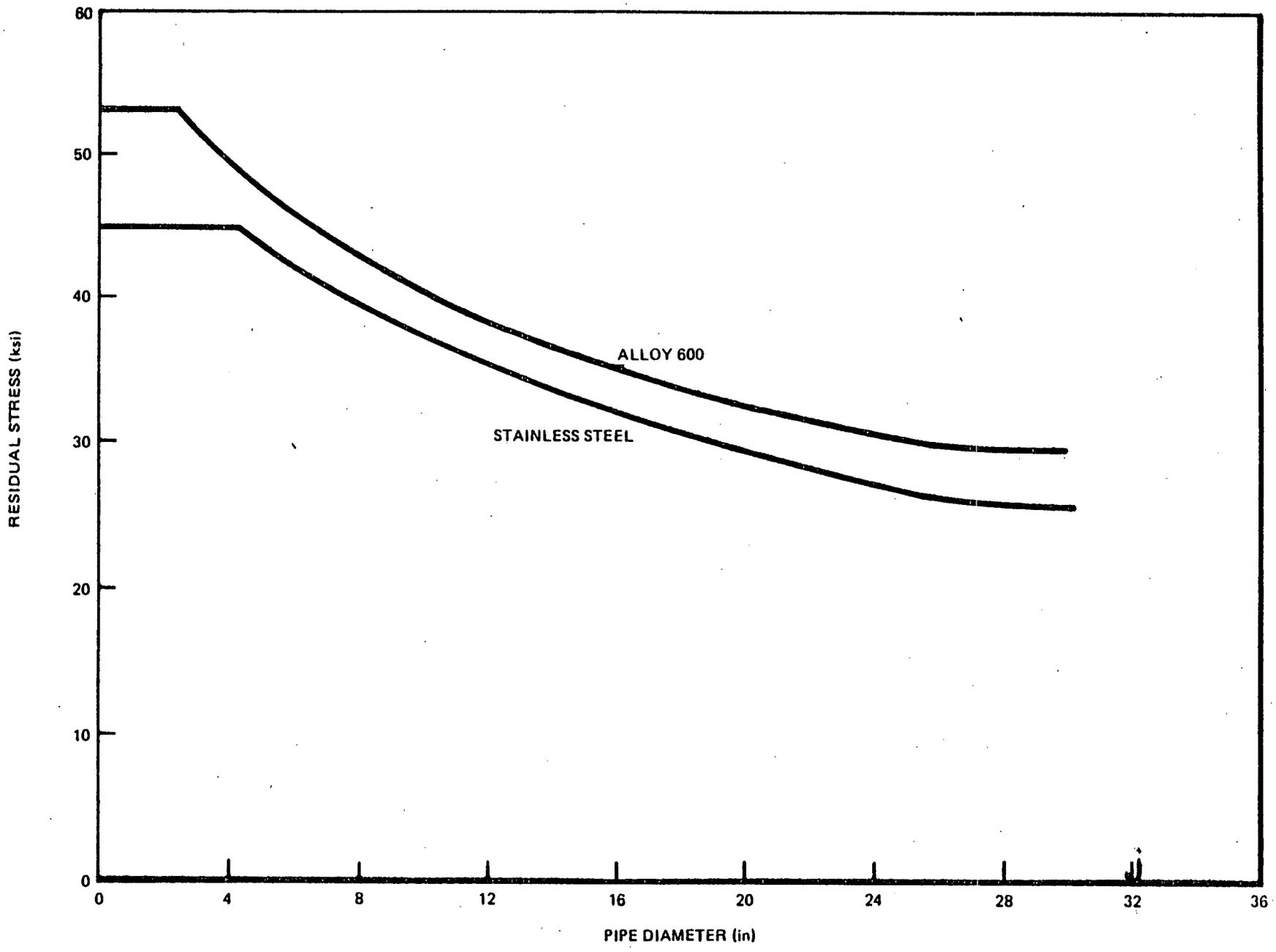

Figure III.B.2-6. Stress Rule Analysis Curve for Weld Residual Stresses

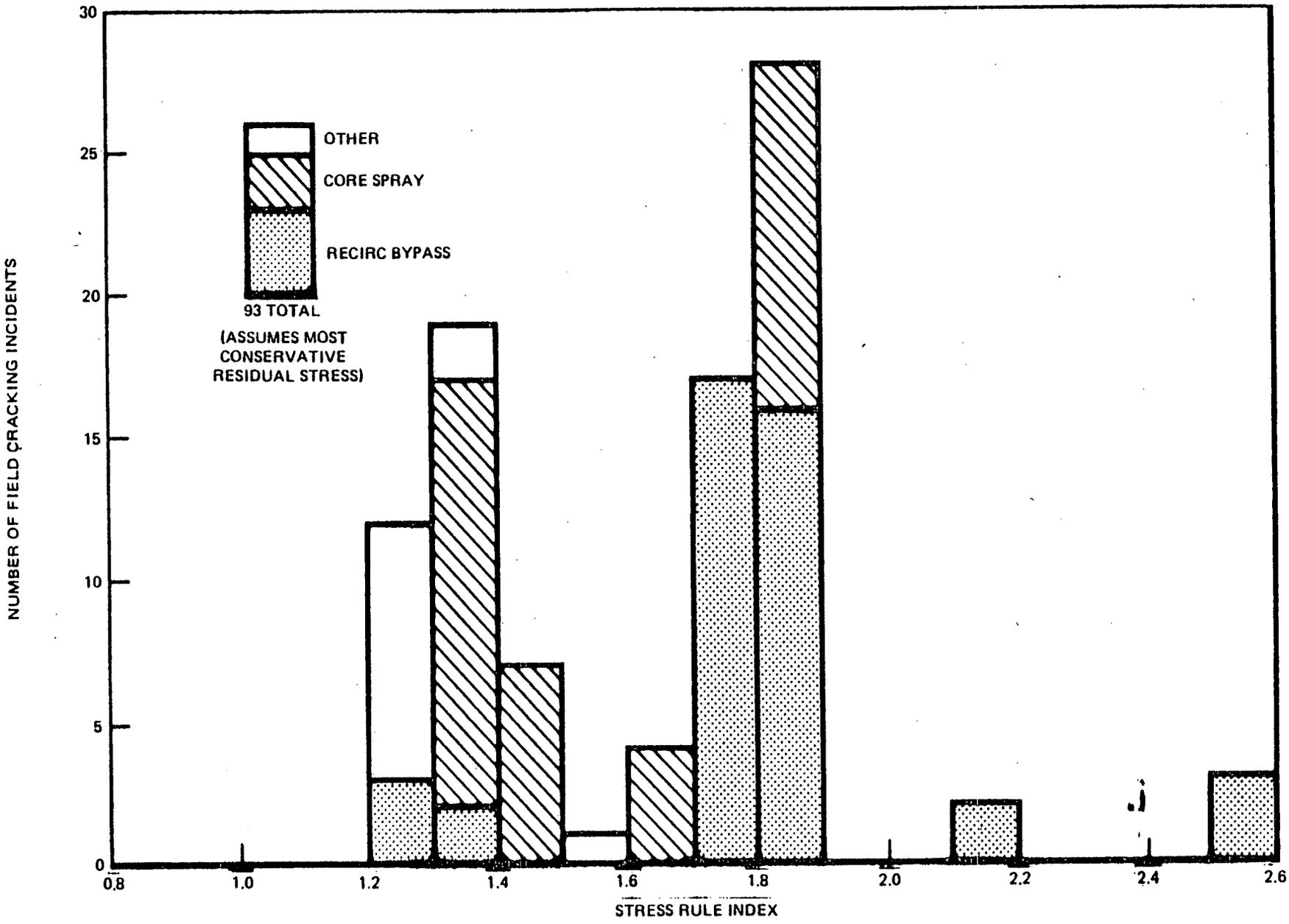

Figure III.B.2-7. Summary of Field Cracking Incidents by Stress Rule Index

ROLE OF RESIDUAL STRESS IN DUANE ARNOLD ANALYSIS

- RELATIVELY HIGH PRIMARY, SECONDARY AND PEAK LOADS ARE APPLIED AT THE CREVICE TIP

- THESE ARE EVALUATED AS FOLLOWS:

PRIMARY + SECONDARY + PEAK + RESIDUAL = STRESS RULE INDEX

0.78 + 0.07 + 0.93 + 0.46 = 2.24

Figure III.B.2-8

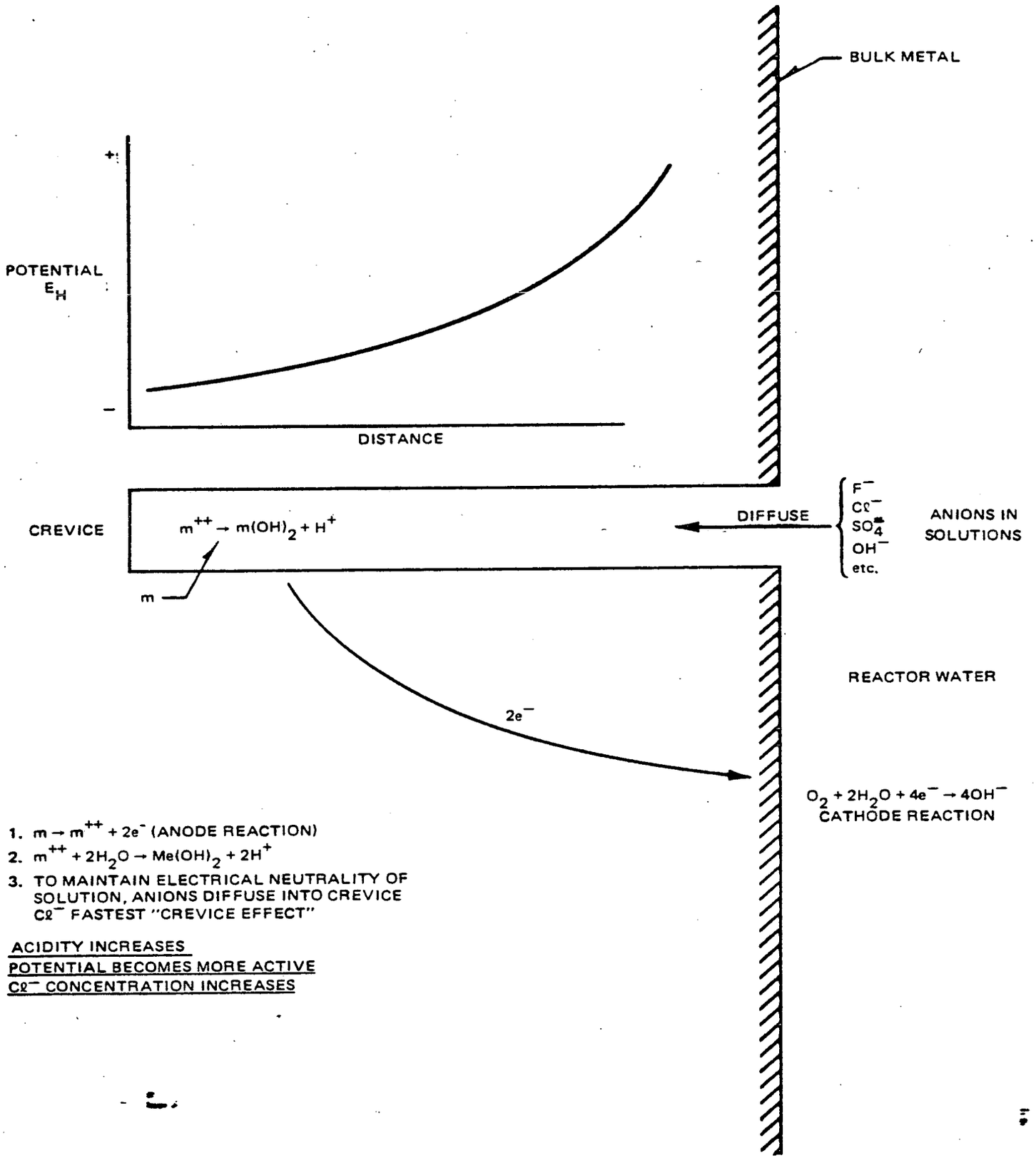

Figure III.B.2-9. Crevice Cracking Mechanism

III.C.1 Description

The configuration of the replacement safe-end is shown in Figure III.C.1-1. The safe-end functions as a transition piece between the nozzle and the piping. It is also the attachment point for the internal thermal sleeve which primarily functions to direct the recirculation flow into the jet pump riser. The welded attachment of the thermal sleeve prevents leakage into the nozzle and thermal sleeve annulus.

The safe-end configuration moves the thermal sleeve attachment weld from the primary pressure boundary. The radius at the pressure boundary eliminates the sharp discontinuity at the junction location. This configuration also contains an extended land weld prep at the thermal sleeve attachment end which acts as a backing ring for the attachment weld. It also provides an adjustment feature to accurately position the thermal sleeve during installation.

The safe-end configuration at the nozzle attachment end improves in-service inspection access at this location. The straight inside and outside surfaces at this attachment simplify ultrasonic angle beam examinations.

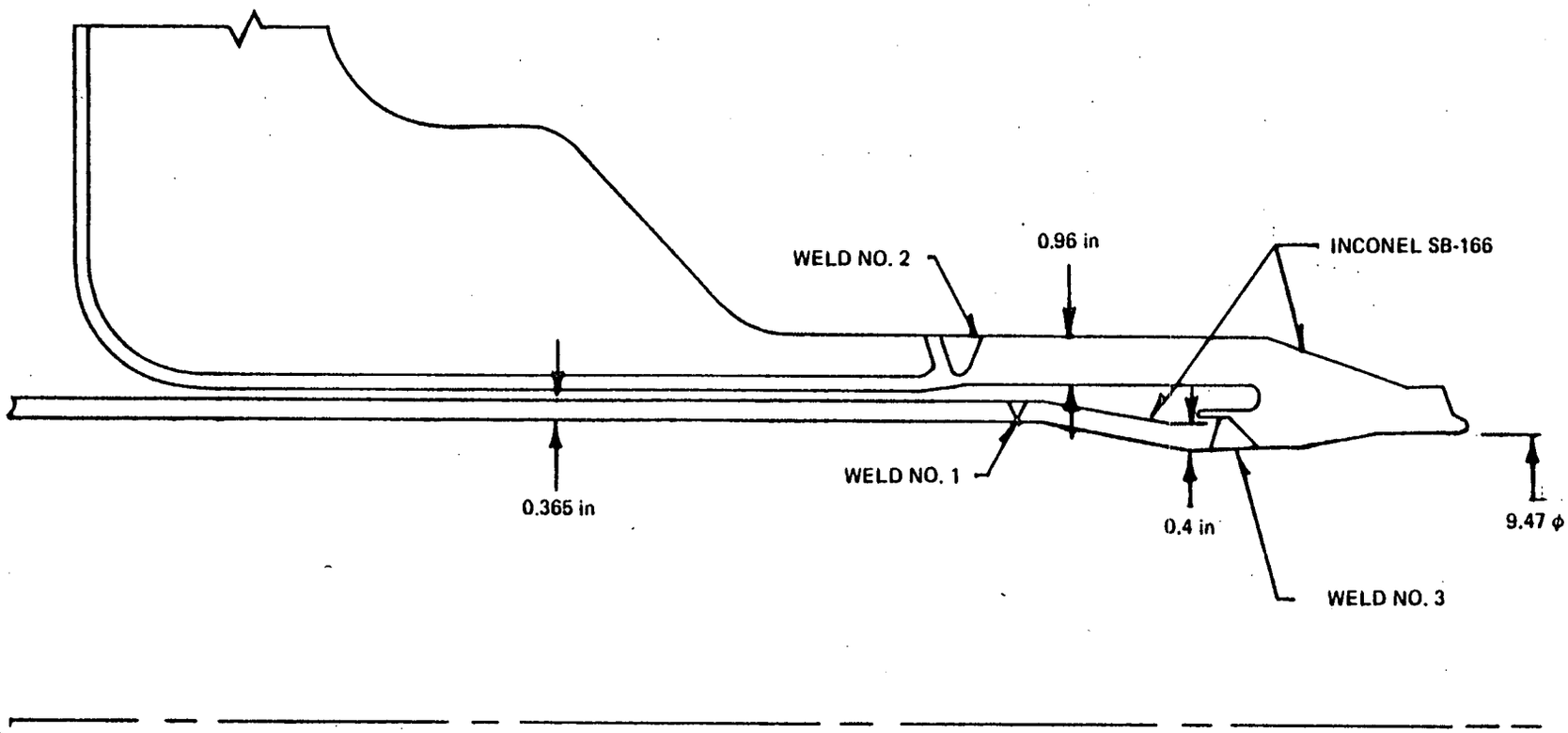

FEATURES:

- ATTACHMENT WELD REMOVED FROM PRIMARY PRESSURE BOUNDARY
- ELIMINATES SHARP DISCONTINUITY AT PRIMARY PRESSURE BOUNDARY
- WALL THICKNESS INCREASED
- FACILITATES FIELD INSTALLATION
- IMPROVED INSPECTABILITY OF PRIMARY PRESSURE BOUNDARY WELDS

Figure III.C.1-1. DAEC Replacement Safe Ends

III.C.2 Fabrication

The material of the replacement safe-end and thermal sleeve adapter is SB-166 (Alloy 600) which is compatible with the existing Ni-Cr-Fe weld butter on the end of the low alloy steel nozzle and the SB-166 thermal sleeve. Since the stainless steel pipe also has Ni-Cr-Fe SB-166 material on the end of the pipe, there are no dissimilar metal welds in the replacement safe-end installation. The replacement safe-end material was supplied in accordance with Section III of the ASME Boiler and Pressure Code, 1977 Edition, with addenda to and including Summer 1977. The thermal sleeve adapter material was supplied using available forgings in accordance with ASME Section III, 1974 Edition, with addenda to and including Winter 1975. All forgings meet the ASME Code material requirements and passed all required examinations.

III.C.3 Stress Comparison to Original Safe-end

An objective of the replacement safe-end configuration is to minimize the susceptibility to IGSCC. The most susceptible region in the original safe-end was at the high stressed safe-end to thermal sleeve attachment. The replacement safe-ends reduce stresses in this region because of the following features:

1. Moving the thermal sleeve attachment weld from the primary pressure boundary removes the weld residual stresses from that region.

2. Eliminating the sharp discontinuity reduces peak stresses in this region.

3. Increasing the wall thickness reduces primary stresses.

Figure III.C.3-1 contains a stress comparison of the replacement with the original safe-end at the crack location which shows a significant improvement in stresses in this region. To determine the susceptibility to IGSCC, a stress index evaluation was performed at this location. A

value of 0.73 was calculated. This is a significant improvement from the 2.24 value calculated for the original safe-end.

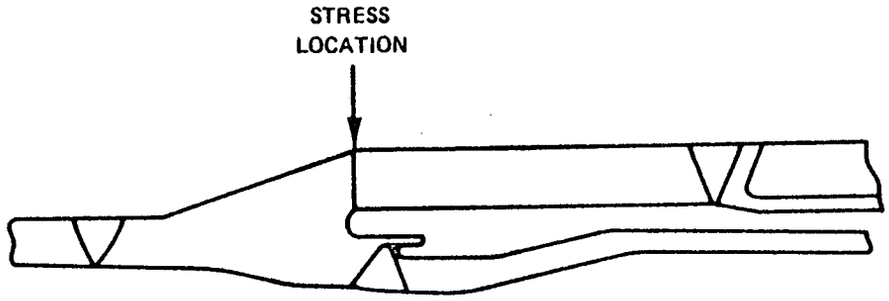

REPLACEMENT SAFE END

STRESS LOCATION	STRESS CATEGORY		
	PRIMARY LOCAL + BENDING (ksi)	PRIMARY + SECONDARY (ksi)	FATIGUE USAGE
	9.4	35.3	0.15

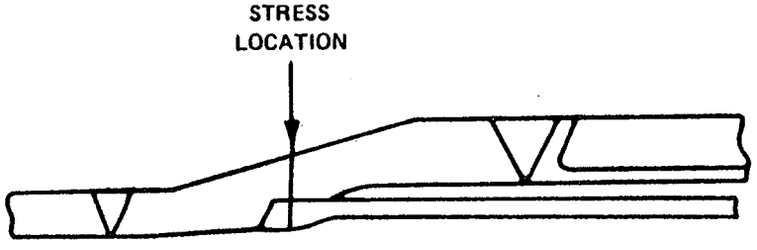

ORIGINAL SAFE END

	18.0	103	0.52

Figure III.C.3-1. Stress Comparison

III.C.4 Stress Indices at Weld Locations

Stress index values were also calculated at all the weld locations in the replacement safe-end assembly using the weld sequence numbers shown in Figure III.C.4-1. The following are the calculated stress index values:

Calculated Stress Index Values

	Stress Index Values				
Weld Location	Primary	Secondary	Peak	Residual	Total
1	.40	0	0	.46	.86
2	.20	0	0	.46	.66
3	.24	0	.14	.46	.84
4	.51	0	0	.52	1.03
5	.35	.16	0	.53	1.04

All the stress index values for the welds associated directly with the safe-end have been reduced to less than 1.0. This has substantially reduced the potential for IGSCC in the safe-end. Even in the two closure welds, welds #4 and #5, the stress indices are approximately 1.0. Since all previous

cracking incidents have occurred at values greater than 1.2, even at these two locations the risk of IGSCC is small. Weld #4 is identical to the weld on the original safe-end attachment for which no indication of IGSCC was found. The stress index value for weld #5 would indicate that its performance would be comparable to weld #4. This provides further support for the acceptability of these welds.

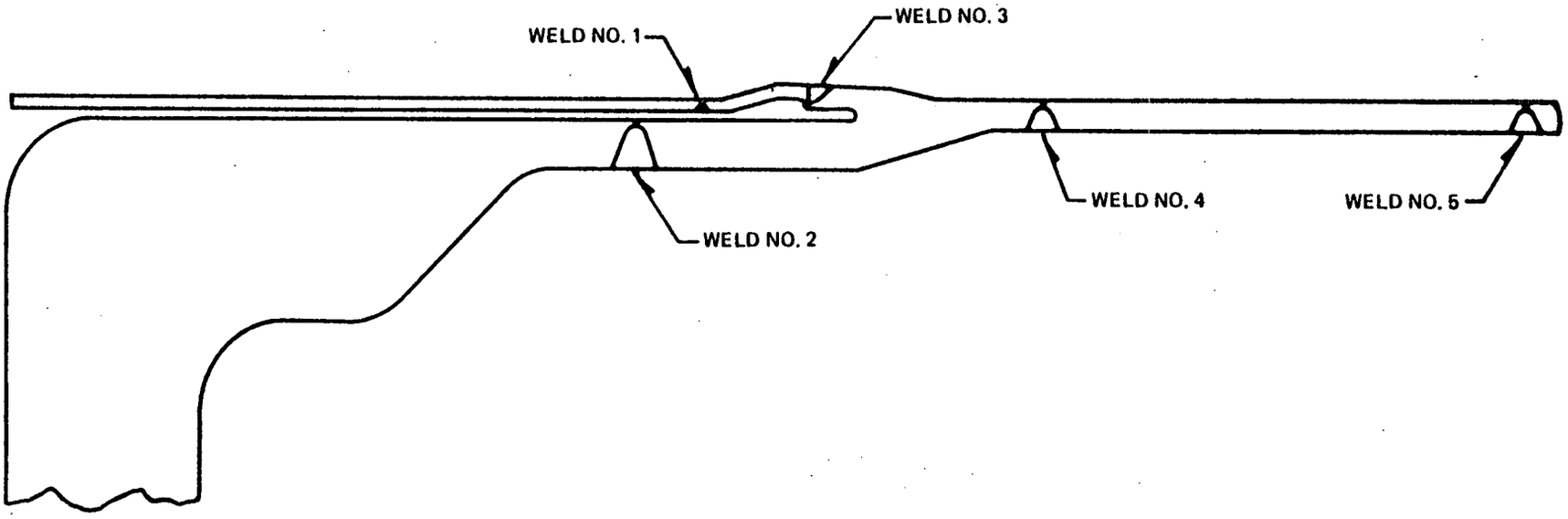

Figure III.C.4-1. Weld Sequence for Replacement Safe End Assembly

III.C.5 Evaluation of Annulus Flow

General Electric has carried out a test program to determine the water exchange rate in the annulus formed by the recirculation inlet nozzle and the thermal sleeve. These tests were performed in a quarter scale clear plastic model of the recirculation inlet nozzle. The total obstruction angle of the three alignment lands was 60°. The results of this study indicate that the whole annulus is flushed in two minutes for a 0.1 inch annulus gap and in five minutes for a 0.032 inch gap. When the above results are extrapolated to the full scale reactor condition, the annulus flushing time will be less than eight minutes for a 0.40 inch annulus gap and less than twenty minutes for a 0.13 inch gap typical of the DAEC annulus. Therefore it is concluded that the annulus is not a crevice.

III.C.5.a Test Conditions

Figure III.C.5-1 shows the overall view of the test setup. It shows a flow control valve, a flow meter in the middle of the test setup, a riser pipe and a thermocouple, a pressure gauge, fill lines, and a quarter scale clear plastic model simulating the recirculation inlet nozzle annulus. Also shown is a digital timer to indicate the elapsed time. Flow patterns were recorded by motion pictures taken after dye was injected at several locations in the annulus.

Table III.C.5-1 shows the comparison between the test conditions and the reactor conditions. In the flow simulation of the annulus, the Reynolds number is the most important parameter. The Reynolds number representing the external flow was 10,000 in the test condition and is 300,000 in the reactor condition. Since both of these Reynolds numbers are in the turbulent flow regime, these two conditions represent the same external flow pattern (Reference III.C.5-1).

Table III.C.5-1. Comparison between test conditions and reactor conditions.

	Test	Reactor
Scale	1/4 scale	Full scale
Water temperature	70-90°F	550°F
Pressure	14.7 psia	1000 psia
Land angle	60°	62.5°

	Test	Reactor
Annulus gap	0.1 and 0.032 inch	Full scale
External flow velocity	0.5 ft/sec	0.5 ft/sec
*External Flow Reynolds Number	10,000	300,000
*Annulus Flow Reynolds Number	200 and 600	6000

* External Flow Reynolds Number is defined as (External velocity x Thermal sleeve Outside Diameter/kinematic viscosity), and the Annulus Flow Reynolds Number is defined as (Entrance Velocity x Hydraulic diameter of annulus/ kinematic viscosity).

The Reynolds number representing the flow near the annulus entrance at the test condition varies from 200 to 600, and is expected to have laminar flow throughout the whole annulus. At reactor conditions, on the other hand, the Reynolds number representing the annulus flow near the annulus entrance is approximately 6,000, and it is believed that the flow starts as turbulent flow near the entrance and becomes laminar flow before it reaches the safe end. Thus it is expected that there will be less friction and more mixing at reactor conditions, and that the flushing time at reactor conditions will be shorter than that extrapolated from the test condition using the scale factor.

III.C.5.b Test Results

The test results are shown in Figure III.C.5-2. It shows the flow patterns observed in the motion pictures. The time required to flush out all the dye injected into the annulus was two minutes for the 0.1 inch annulus gap and five minutes for the 0.032 inch gap. It was also observed that flushing time or water exchange rate in the annulus was essentially independent of the orientation of external flow with respect to the lands.

The flow pattern is expected to be similar between the quarter and full scale. The time required to flush the annulus will be four times longer in reactor than in the quarter scale test model, because the length scale becomes four times longer yet velocity stays the same. The reactor condition, however, is expected to produce higher velocity and shorter flushing time as discussed at the end of III.C.5.a. Therefore, the flushing time for reactor condition will be less than eight minutes for 0.4 inch annulus gap and less than twenty minutes for 0.13 inch annulus gap.

III.C.5.c Annulus Water Chemistry

A conventional description (Reference III.C.5-2) of a crevice is a geometric condition in which dissolved oxygen has been depleted, and acidity and non-hydroxyl anions increase. From the work performed at General Electric Corporate Research and Development Laboratory by Taylor (References III.C.5-3&4), a relationship between flushing rate and crevice acidity was developed. Crevice acidity will increase when non-hydroxyl anionic impurities such as chloride (or its equivalent) is present. Figure III.C.5-3 is a graphical representation of the acidity (pH) versus water exchange rate in the annulus under normal BWR operating conditions using a maximum non-hydroxyl anion concentration of 0.25 ppm. During normal BWR operation, the maximum allowable concentration of non-hydroxyl anion is 0.2 ppm (Normal Water Quality Specification). The flushing times of less than 8 minutes and less than 20 minutes identified by the flow visualization tests correspond to greater than 180 turnovers and greater than 72 turnovers per day, respectively. From Figure III.C.5-3 it can be seen that acceptable water chemistry, i.e. neutral pH conditions; exist for turnover rates as low as one turnover per day. Consequently adequate flow exists in the DAEC annulus to maintain acceptable water chemistry.

REFERENCES

SECTION III.C.5

(1) Schlichting, H., Boundary - Layer Theory, Sixth Edition, McGraw-Hill Book Company, 1968, pp. 18, 31 and 32.

(2) J. W. Oldfield and W. H. Sutton, Br. Corros, J 13, Vol. 13 (1978)

(3) D. F. Taylor, Corrosion/78, Paper No. 199. To be published in Corrosion.

(4) D. F. Taylor, Corrosion/79, Paper No. 93. To be published in Corrosion.

FIGURE III.C.5-1

TEST SET-UP

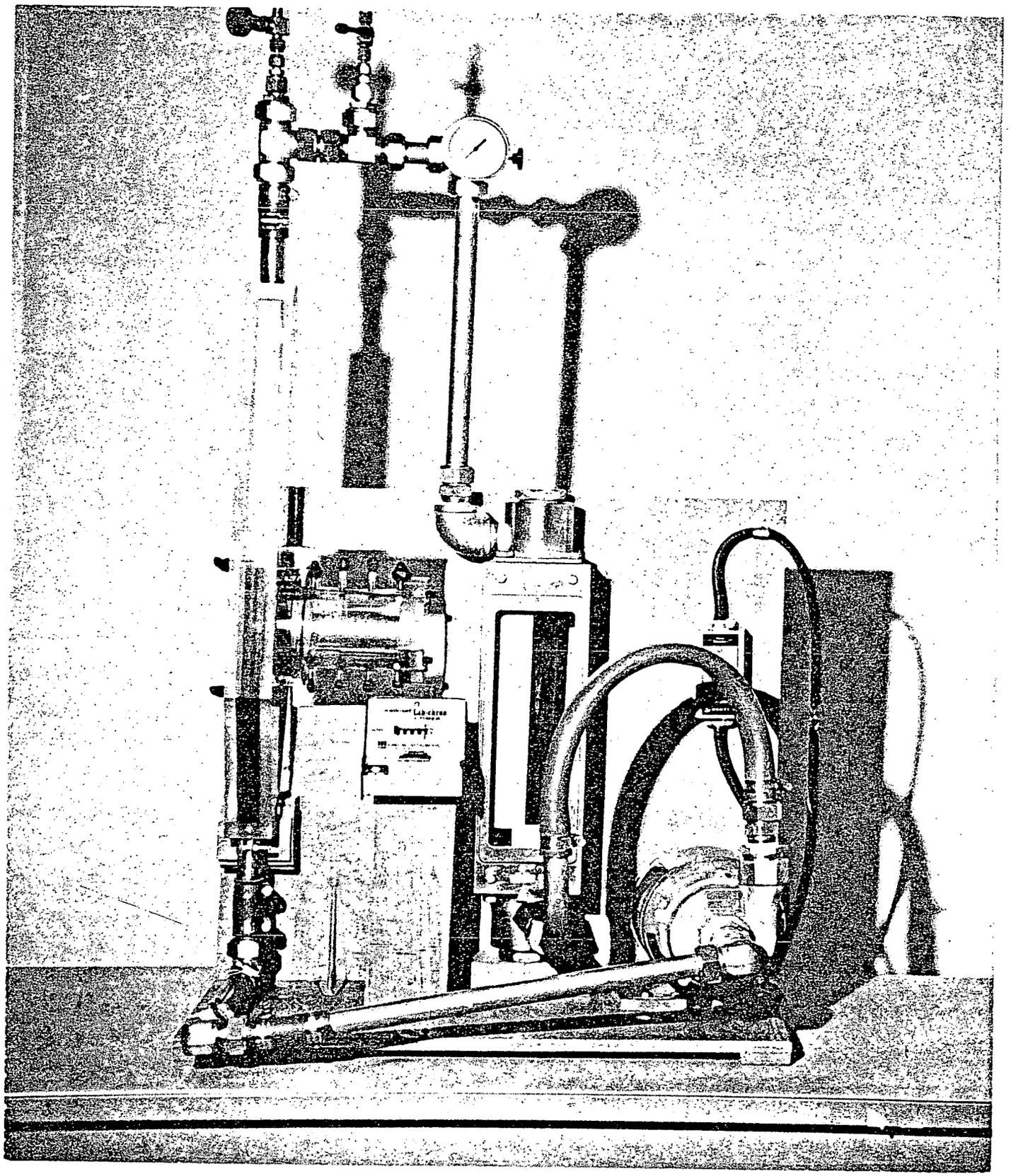

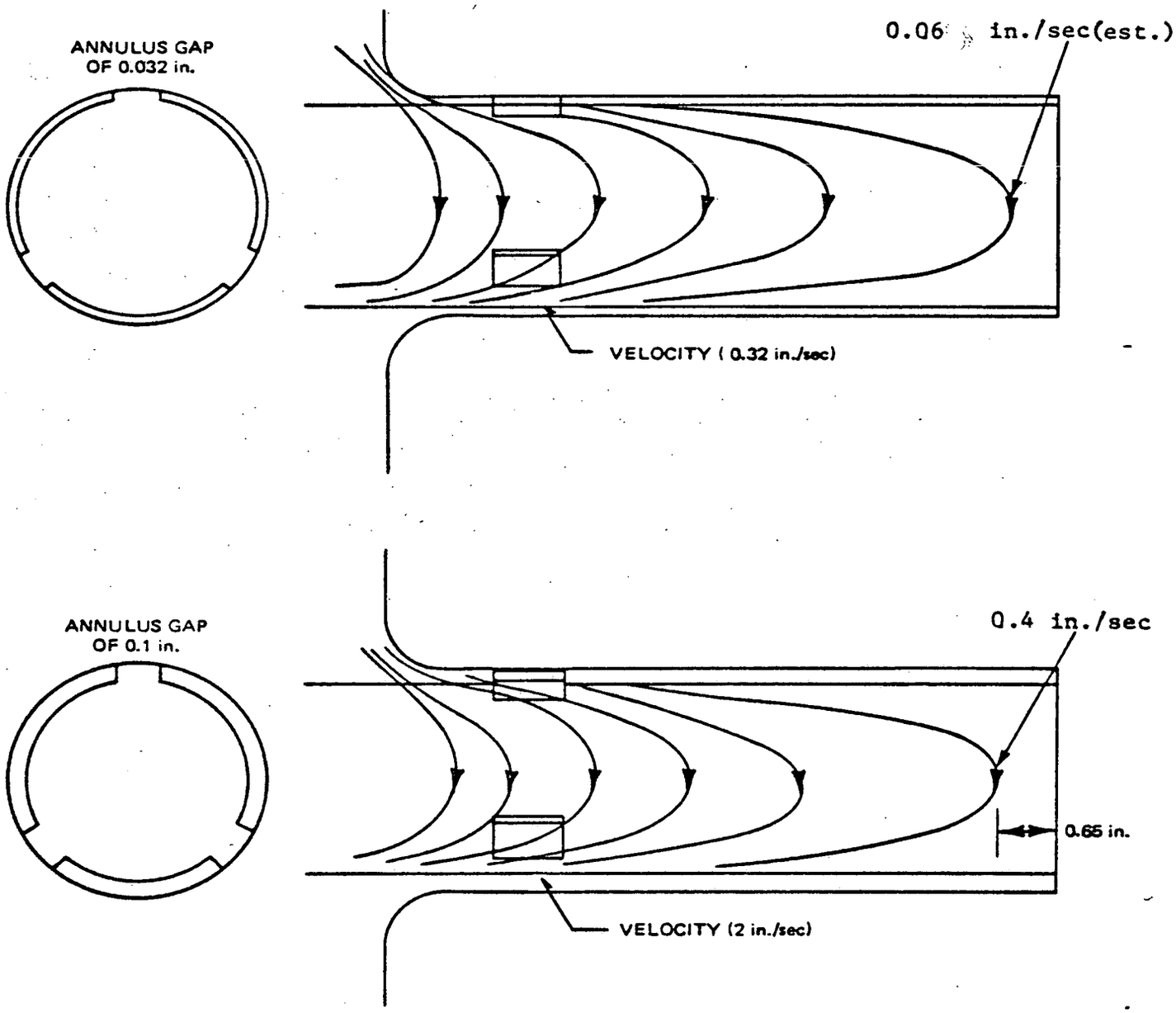

Figure III.C.5-2. Flow Pattern in the Recirculation Inlet Nozzle Annulus

DUANE ARNOLD ANNULUS EVALUATION

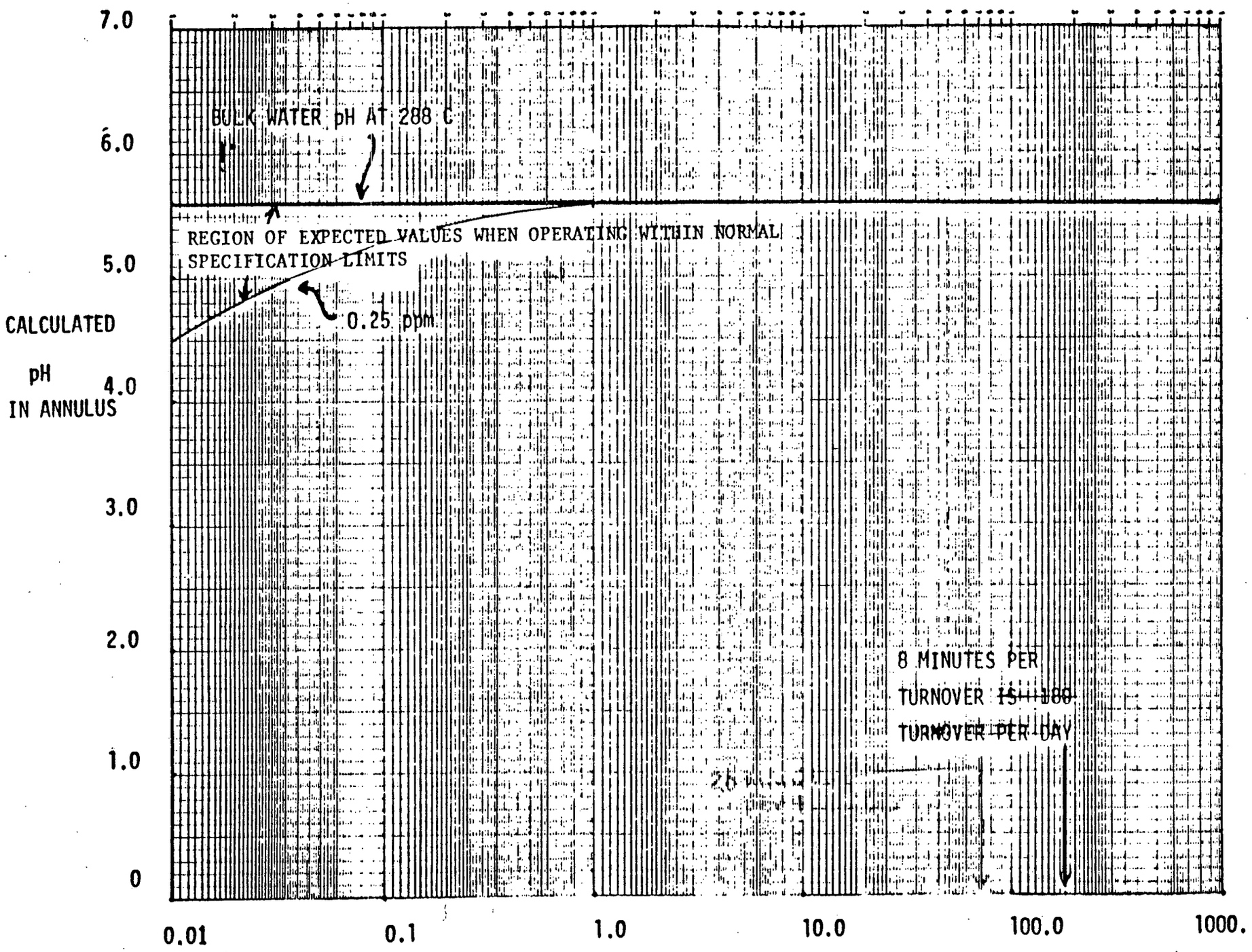

WATER EXCHANGE RATE IN ANNULUS

Figure III.C - 3

III.C.6 Vibration/Hydraulics

To utilize the replacement configuration on the recirculation inlet safe end, it was necessary to have a small local area reduction at the attachment location of the safe end and thermal sleeve. Because of various geometric interfaces, local area variations are common on nozzles with thermal sleeve attachments. For this nozzle the change in head loss is less than 0.5 ft., which results in a less than 0.1% core flow reduction which does not exceed the calculated available core flow margin. Actually, small unidentified head losses, such as this local reduction, were originally anticipated and excess core flow capability was designed into the recirculation system.

An evaluation has also been completed to determine if the local area reduction in the safe end to thermal sleeve attachment has any effect on vibration. This evaluation was performed by comparing the original DAEC vibration data with another operating plant wich has a similar geometry as the replacement safe end configruation. In calculating the associated head loss for the other plant it was noted that it was greater than the DAEC replacement safe end configuration.

The stresses at this attachment location are computed by using the available vibration data and a representative computer model of the jet pump system. These results show

no detectable change in vibration from the local area changes. This result was anticipated since the area change occurs near a rigid attachment.

In conclusion, the replacement safe end has a negligible effect on the hydraulics and vibration of the recirculation system.

III.C.7 Adequacy of Alloy 600 Material

Alloy 600 material (SB-166) is suitable as the replacement safe end material for several reasons. From a design viewpoint, Alloy 600 is a high strength material. Operating plant experience and laboratory data substantiates that Alloy 600 is an acceptable safe end material even with the presence of a crevice in a weld heat affected zone under low sustained stress conditions. Alloy 600 also has thermal characteristics which are compatible with both the low alloy steel nozzle and stainless steel pipe materials.

From a fabrication and installation perspective, Alloy 600 is an ideal material for the DAEC application, since it was readily available and all the existing weld attachment locations contain Ni-Cr-Fe material which avoids having dissimilar metal welds in the field.

Alloy 600 has also demonstrated that it is a proven material in the BWR environment since no previous failures have occurred in this material. Alloy 600 material has been used in various pressure boundary applications for nearly all of the BWR operating plants. Some of the early BWR designs have had excellent service from Alloy 600 pressure boundary components for 15 years. Also, Ni-Cr-Fe weld material has been commonly used in BWR's for attaching stainless steel

safe ends to low alloy steel nozzles for more than eight years. Additionally, two operating plants have operated from 6 to 8 years using Alloy 600 safe end material in a similar configuration with good service experience.

One example is the Alloy 600 thermal sleeve weld in the feedwater nozzle of an overseas GE-BWR where cracking has not been observed. The weld configuration consists of an Alloy 600 thermal sleeve welded to an Alloy 600 nozzle with a severe creviced condition (Figure II.C.7-1). After ten years of operation, this nozzle was inspected, utilizing radio graphic and dye penetrant, ultrasonic testing methods, and no cracking was observed at the weld.

Although no detailed stress values are available for the creviced location, an evaluation recently performed by General Electric indicates that the stresses were likely to be moderately high in this area. It is estimated that the stress rule index is approximately 1.2, which is significantly lower than the 2.24 value calculated for the DAEC case. The significance of this particular thermal sleeve weld information is that it represents a successful use of Alloy 600 weld even with a severe crevice over a relatively long service period.

Based on the above information, Alloy 600 is an acceptable material provided the sustained tensile stresses are not excessive.

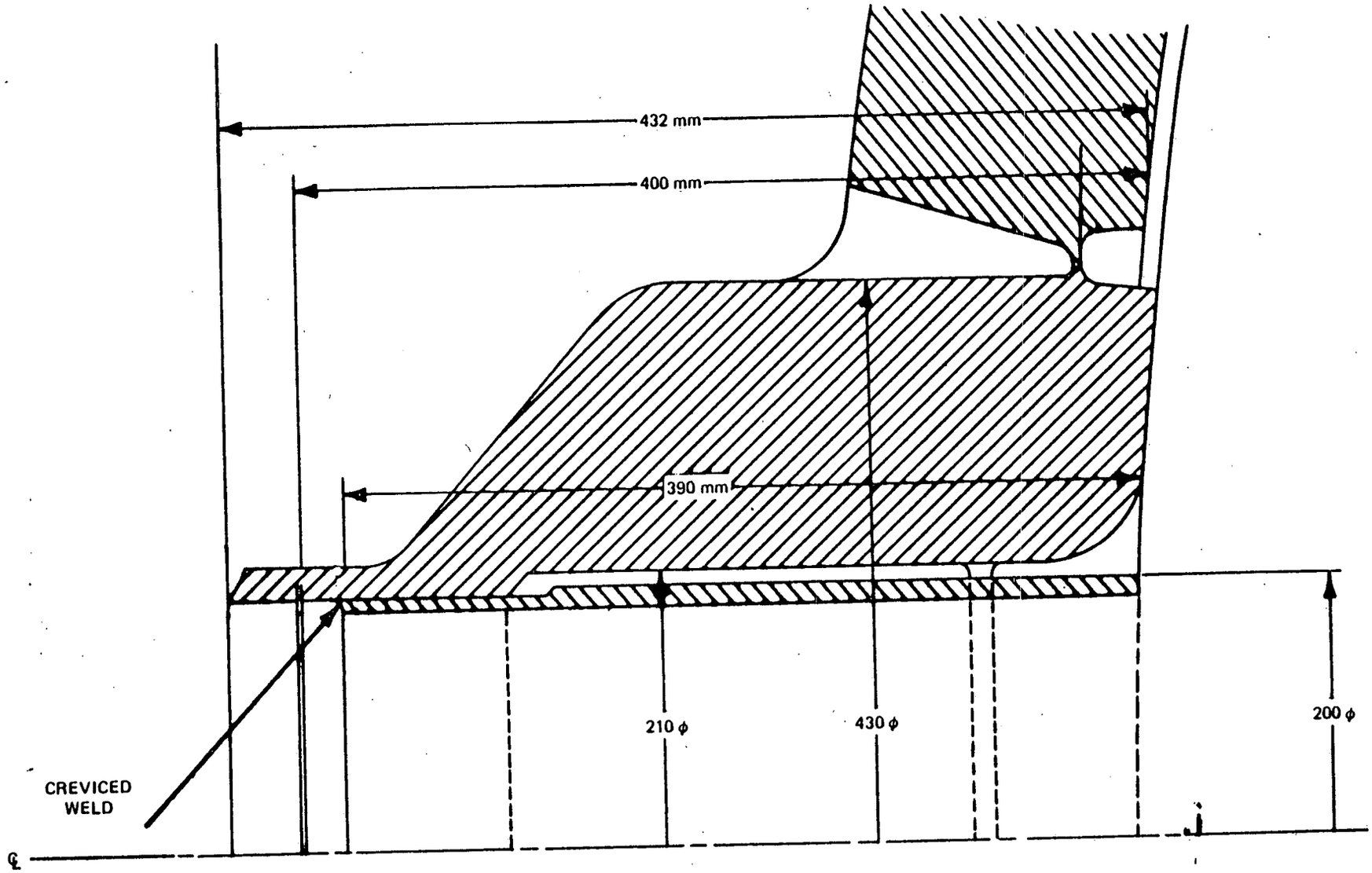

Figure III.C.7-1. Overseas Feedwater Nozzle

III.C.8.a. Thermal Sleeve to Safe End Weld

The configuration of the thermal sleeve attachment weld to the safe end (Weld #3) as shown in Figure III.C.4-1 was selected to facilitate field installation and minimize personnel exposure. An important objective during installation is to position the thermal sleeve close to its original position so that the function of the jet pump assembly is not affected. The critical time for positioning the thermal sleeve is during the fitup of Weld #3. At this time, the root gap of the Weld #3 configuration is adjustable and enables the thermal sleeve to be precisely positioned. Also, since this weld prep configuration does not require a precise fitup, radiation exposure to workers is minimized. The backing ring design was selected for Weld #3 as the best alternative to successfully accomodate the field conditions, radiation levels, and the variables affecting hardware fitup and positioning.

An Alloy 600 thermal sleeve to safe end weld joint similar to the DAEC replacement configuration was examined by General Electric in a welding mockup test performed in 1975. This work was performed for feedwater connections for plants under construction. This weld joint design was evaluated by welding mockup tests. It was a backing ring weld joint design, as shown

in Figure III.C.8-1. The welding tests were conducted to determine whether the joint design could be readily welded. The backing ring weld was designed for ease of fitup and welding and not specifically for full fusion or penetration. The backing ring will tolerate greater alignment differences between the thermal sleeve and safe end in the axial direction, which is important to simplify installation of a new safe end on a plant where the thermal sleeve is already installed. The backing ring weld is also much easier to make in comparison to other potential joint designs. Although it was not possible to demonstrate good penetration around the entire circumference,the results from the feedwater program weldability mockups indicate that this type of weld can be made.

Since the back side of Weld #3 cannot be inspected to establish if full weld penetration has been achieved, and since the potential for a crevice exists if the extended land distorts toward the thermal sleeve adaptor during welding, it is assumed in the stress evaluation that the potential for a crevice exists. However, one welding objective was to attempt to penetrate as much as possible to minimize crevice conditions. To reduce the concern regarding this assumed condition, the wall thickness was increased as much as practical to reduce

primary stresses from hydraulic loads, thereby minimizing the stresses. As reported earlier, the stress index value at this location is 0.84 which was determined using design loads and pressures. Since the design values are conservative, a further evaluation using loads closer to the actual hydraulic loads and operating pressures was completed. For these loadings, a stress index value of .66 was calculated. Another conservative aspect of the stress index value is that the assumed residual stress is an upper bound value applicable to butt welds. It is believed that residual stresses at the root of inside-out welds such as Weld #3 are much lower than the assumed stresses. Since the stress index value is below 1.0 and since all previous cracking incidents have occurred at values above 1.2, the potential for IGSCC is relatively low. Although failure of Weld #3 is unlikely, if a crack occurred, it would be oriented in the circumferential direction since the maximum sustained stresses are in the transverse direction and the weld heat affected zone is circumferential. The predominate stress sources are the hydraulic loads and the weld residual stresses. Cracking in the axial direction is extremely unlikely since hoop stresses are small. Therefore, the primary pressure boundary would not be affected since cracks would not propagate to this region.

Assuming a complete failure of Weld #3 in the circumferential direction, the following consequences have been evaluated.

Under these circumstances, structurally there would be no axial restraint provided on the thermal sleeve. Assuming that the reactor is at normal rated conditions with nominal clearance between the thermal sleeve and the nozzle centering pads, the thermal sleeve could move radially inward approximately two inches (conservatively neglecting pad friction and jet pump diffuser stiffness). Yielding would occur in the jet pump riser elbows and the riser brace which permits the deflection. The maximum stress in the diffuser would be below the normal allowable value. Other than the riser elbow and brace local yielding, no damage would be expected on the reactor vessel or internals, in no case is the primary pressure boundary integrity compromised.

Jet pump performance would be affected since some recirculation flow would leak into the vessel through the nozzle and thermal sleeve annulus. By an area ratio comparison, flow in the two affected jet pumps would drop to approximately 76% of rated flow, which produces a reduction in actual and measured core flow of approximately 3%. The reduction in jet pump flow

would be detected in the control room by the core flow measurement indicators. Normal technical specification requirements on jet pump surveillance would detect such a condition and require reactor shutdown for the case of inoperative jet pumps.

Plant operation resulting from the 3% reduction in core flow would be manifested by a small power reduction (slope of flow control line times delta core flow). Reactor pressure control would compensate to some extent providing stable plant operation at reduced electrical output of approximately 2%. Smaller losses in jet pump flow would have the same general effect but of a lesser magnitude. None of the postulated events pose any threat to public safety or health. In all cases, calculation of operating thermal limits would be unaffected since core flow measurements and process computer correlations would account for the change in core flow. (Reference III.C.8-1).

III.C.8.b. Thermal Sleeve Attachment Weld Residual Stress Analysis

Residual stress analyses of the thermal sleeve to safe end attachment welds were performed at Battelle Columbus Laboratories for both the original and replacement safe end configurations. The method used incorporates transient thermal analysis of a point heat source moving through a body, followed by an axisymmetric, elastic-plastic stress evaluation of the resulting temperature distributions. The analysis is performed as a time history, considering actual welding parameters, such as weld heat input, travel speed number of passes, and utilizing a temperature dependent material stress-strain curve. Figures III.C.8-2 and 3 illustrate the axisymmetric finite element models used for the stress evaluations of the original and replacement safe end configurations, respectively. The shaded area in these models represents the deposited weld metal, which is incrementally added during the analysis to simulate the multi-pass welding process. The initial weld passes are simulated by a temperature transient occurring with the outer rows of weld elements assumed to have zero modulus. As additional temperature transients are applied to represent subsequent weld passes, non-zero modulus

values are assigned to additional rows of elements. This process is repeated until the total number of weld passes to complete the weld have been simulated.

The resulting axial residual stress distributions are illustrated by the contour plots of Figures III.C.8-4 and 5. Figure III. C.8-4 indicates that, in the original safe end configuration, yield level tensile residual stresses exist over the entire safe end side of the crevice, which is consistent with the occurrence of cracking at that location, and with the residual stress value assumed in the Stress Index analysis of the original safe end reported in Section III.B.2 of this report. Compressive residual stresses are predicted, however, on the thermal sleeve side of the crevice, and, as illustrated in Figure III.C.8-5, on the thermal sleeve side of the replacement safe end in the region where a potential crevice may exist due to the presence of the backing ring. If the stress rule index is calculated assuming zero (rather than tensile yield level) residual stress, the resulting stress rule index values are 0.38 for design loads and pressures, and 0.2 for operating loads and pressures.

The analytical techniques described above have been calibrated by comparison to experimental residual stress measurements

on butt-welded stainless steel pipe. The analysis accurately predicts the peak values of measured residual stress on comparable pipe configurations. However, the axisymmetric nature of the analysis precludes any prediction of circumferential variation of residual stress which has been observed in some measurements. While there is the potential for this circumferential variation in the thermal sleeve attachment weld, the fact that the analysis predicts compressive residual stresses at the potential crevice location in the replacement safe end provides further evidence that the stress rule evaluation of that location in Section III.C.3 of this report is conservative.

III.C.8c THERMAL SLEEVE TO SAFE END WELD MOCKUP TEST

A mockup weldability test was conducted on the DAEC thermal sleeve to safe end weld (weld #3). The weldability test simulated the actual environmental conditions encountered in the containment. Welders wore the required anti-contamination clothing and masks, and the weld was conducted in a restricted enclosure.

A section of carbon steel pipe was overlayed with Alloy 600 weld metal and machined to the thermal sleeve adaptor dimensions. Dimensional compatibility was limited to the area of the weld preparation for weld #3. The pipe was then fitted to an Alloy 600 safe end. A minimum root gap at weld #3 was established to demonstrate the most difficult arrangement for weld application.

Weld material was applied to weld #3 utilizing the approved weld procedure. A progressive liquid penetrant examination was performed as each one-third of the weld was completed, using the production procedure.

Weld parameters such as weld shrinkage, welder identification, and welding time were recorded as required by the mockup procedure.

Upon completion of the weld and sectioning, the specimen was etched and examined. It was determined that complete fusion of the lip on the thermal sleeve was achieved at the location examined. Because the root of the production welds cannot be examined to confirm that complete fusion is achieved in every case, the design basis assumes a potential crevice exists at weld #3. Moreover, it was noted from the mockup that some local deformation of the backing ring against the thermal sleeve did occur. This deformation could potentially contribute to a crevice-like condition similar to (but probably less severe than) the crevice assumed in the design basis.

III.C.(8)(d) Thermal Sleeve to Safe End Weld Installation Inspections

The installation and welding goal for Weld #3 was to position the thermal sleeve and related jet pump assembly in its original condition.

The sequence listed below details important steps taken during the completion of Weld #3.

1. Prior to welding, the weld gap at the root of Weld #3 was measured with the thermal sleeve in the relaxed position.
2. Through the use of a positioning device, the thermal sleeve was moved axially inward (towards the reactor vessel), a distance of 1 weld shrinkage value for Weld #3.
3. During weld-up of this weld, a progressive liquid penetrant examination was conducted as each 1/3 of the weld was completed.
4. Upon completion, final witness mark measurements were taken to ensure compliance with the original design requirements.

REFERENCES

III.C.8-1 J. F. Carew, "Process Computer Performance Evaluation Accuracy," NEDO 20340, June 1974.

III.C.8-2 Rybicki, E. F., et al, Residual Stresses at Girth Welds in Pipes and Pressure Vessels, Final Report to U.S. NRC, Div. of RSR, Contract No. AT(49-24) - 0293, NUREG-0376, Nov., 1977.

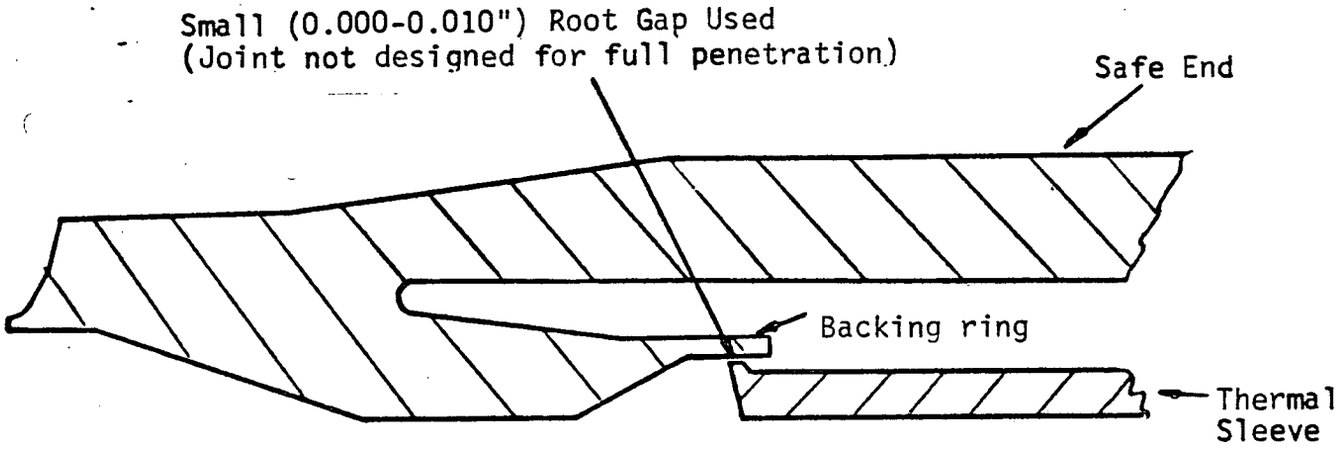

Feedwater Safe End Mockup
Backing ring weld joint design.

Figure III.C.8 - 1

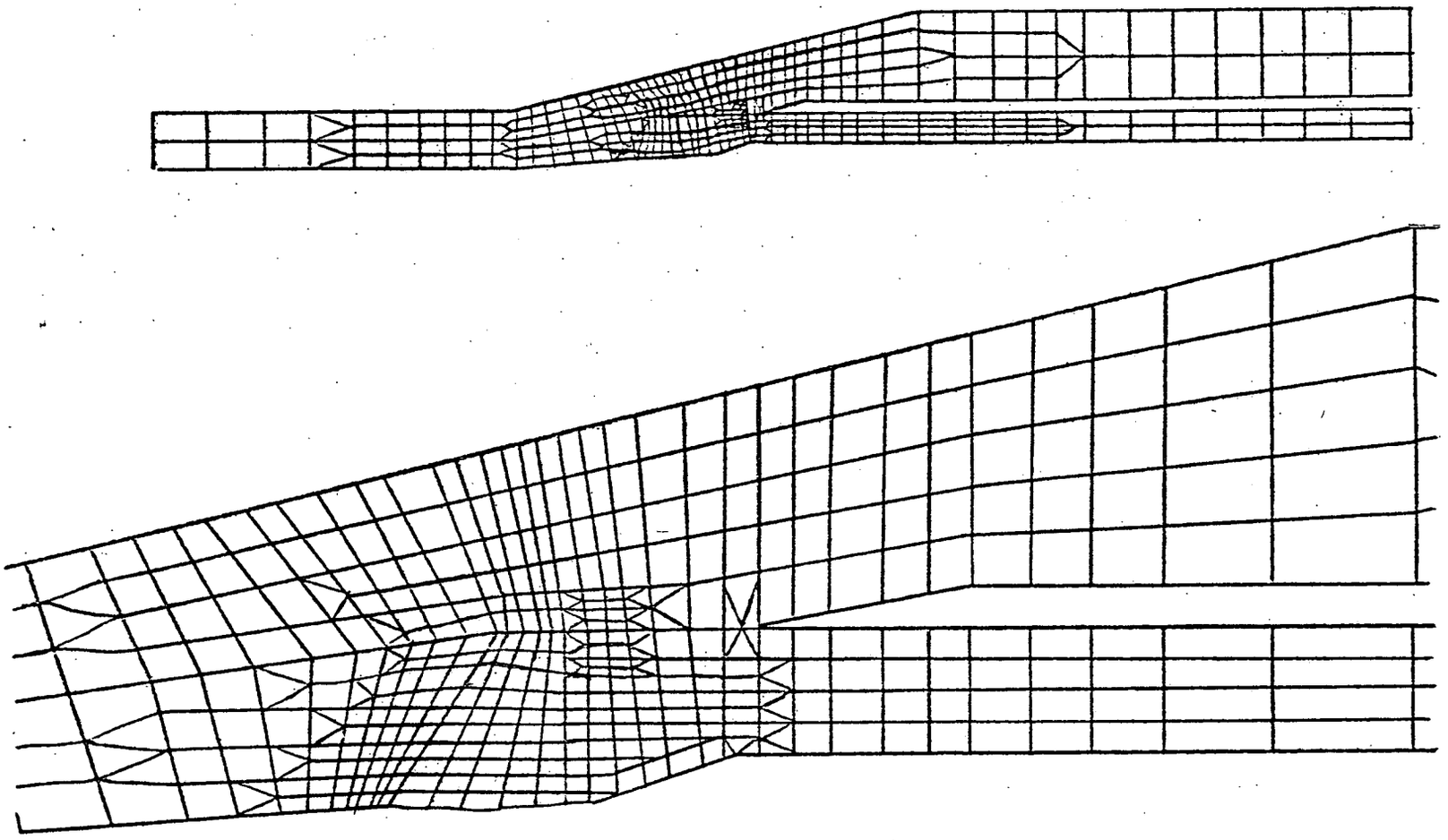

FIGURE III.C.8-2 AXISYMMETRIC FINITE ELEMENT MODEL USED FOR RESIDUAL STRESS ANALYSIS OF ORIGINAL SAFE-END THERMAL SLEEVE ATTACHMENT WELD

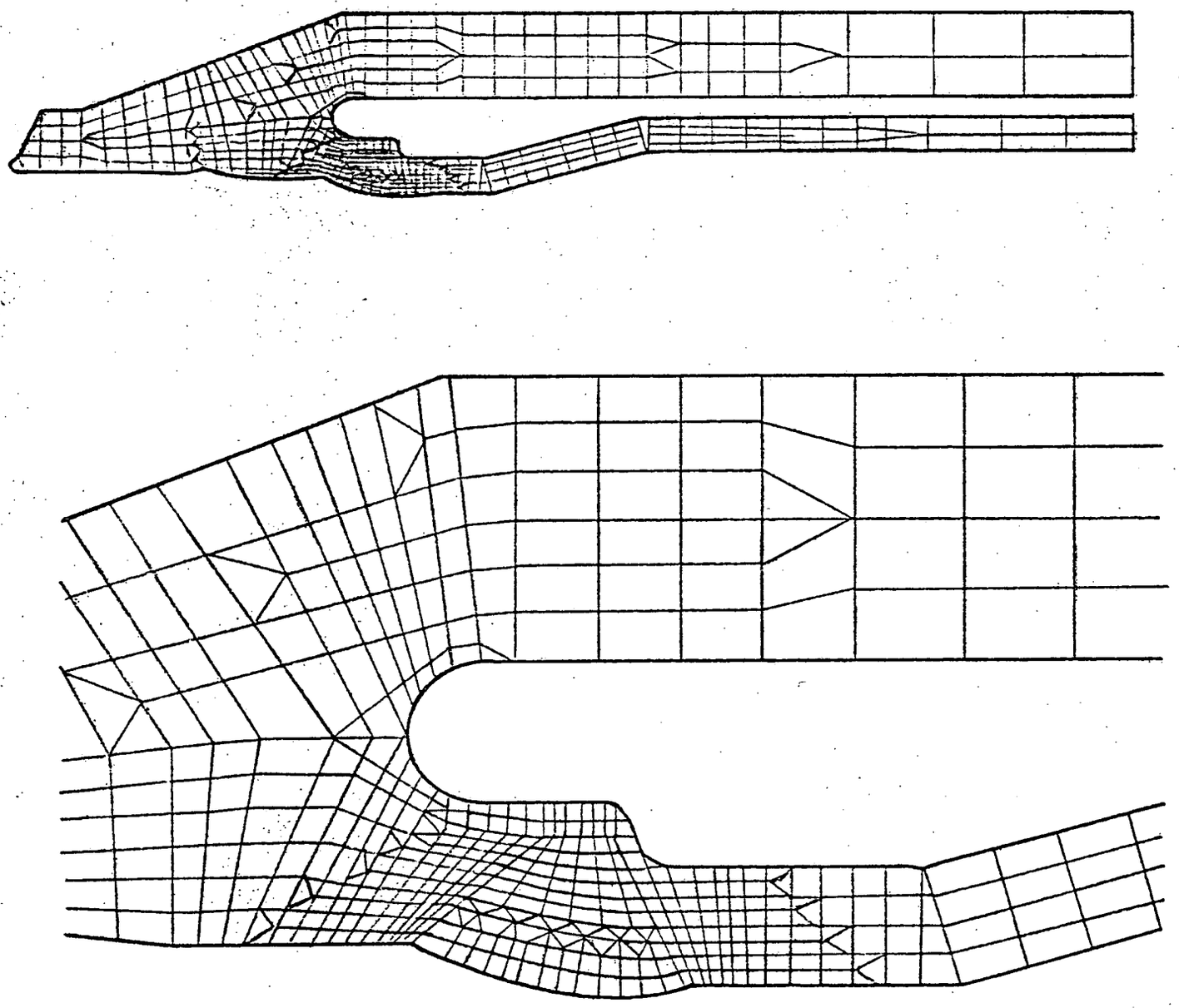

FIGURE III.C.8-3 AXISYMMETRIC FINITE ELEMENT MODEL USED FOR RESIDUAL STRESS ANALYSIS OF REPLACEMENT SAFE-END THERMAL SLEEVE ATTACHMENT WELD (WELD #3)

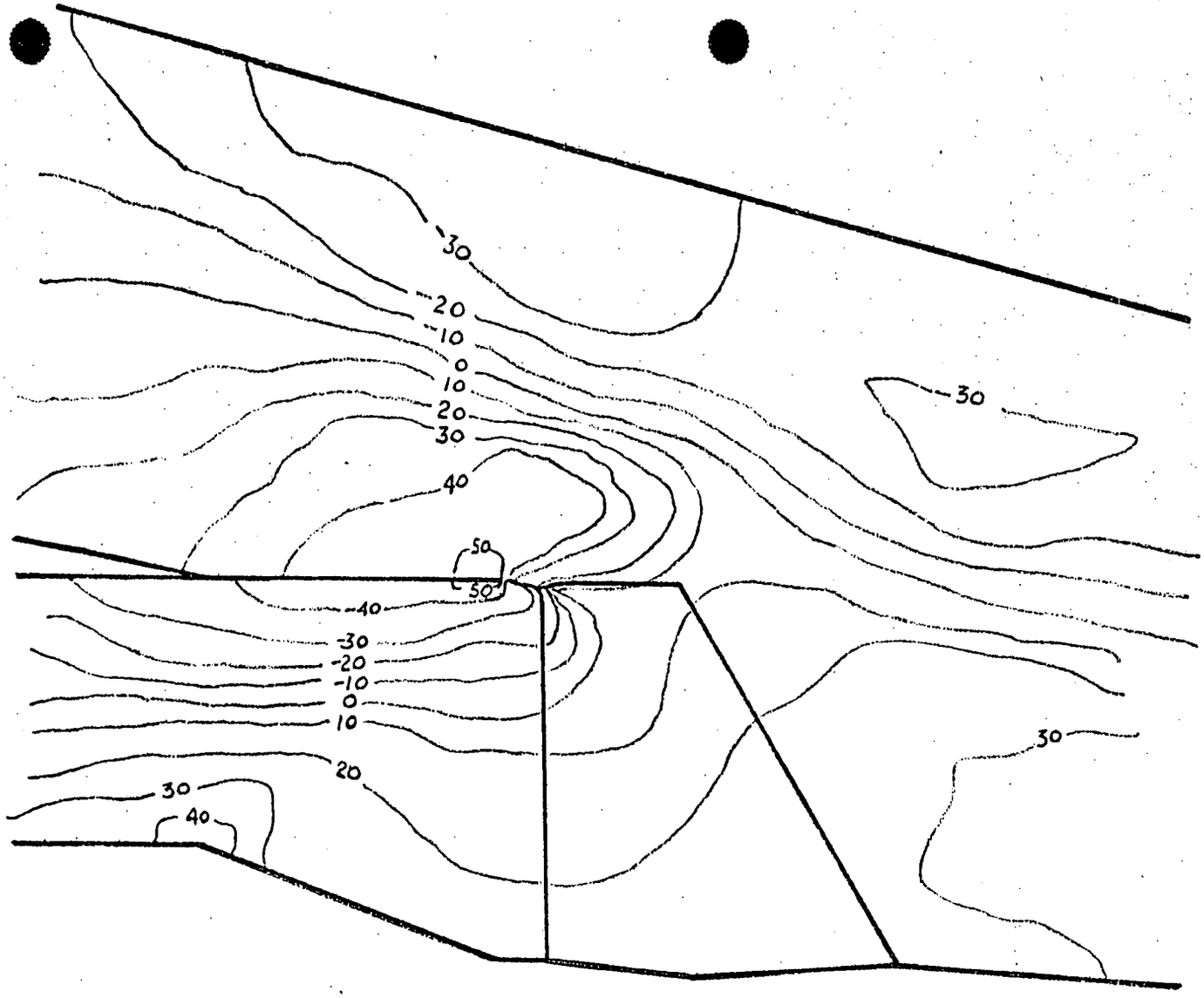

FIGURE III.C.8-4 CONTOURS OF CONSTANT AXIAL RESIDUAL STRESS DUE TO THERMAL SLEEVE ATTACHMENT WELD IN ORIGINAL SAFE-END CONFIGURATION

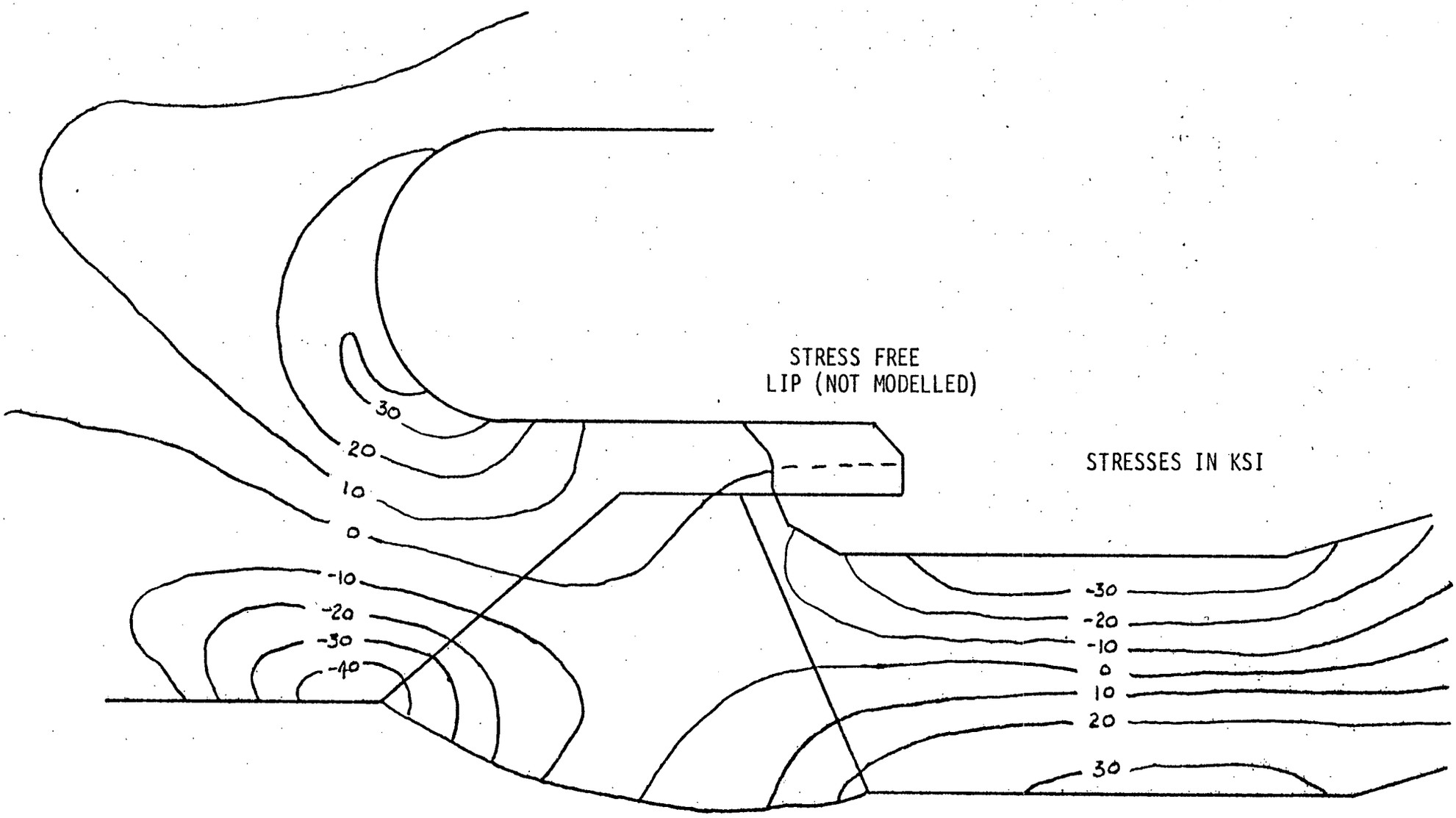

FIGURE III.C.8-5 CONTOURS OF CONSTANT AXIAL RESIDUAL STRESS DUE TO THERMAL SLEEVE ATTACHMENT WELD IN REPLACEMENT SAFE-END CONFIGURATION

III.D REPLACEMENT INSTALLATION

Preparation for the replacement installation of the safe ends required that the recirculation system piping, supports and restraints be inspected. These inspections, conducted at cold shutdown conditions, found no movement restrictions.

Also, inspections originally performed during initial plant startup in 1974 were redone to verify that the recirculation system piping had no restrained movement for thermal expansion and that the pipe supports functioned in the specified manner. Test data was recorded and analyzed for system temperatures of 110°F, 340°F and 545°F. The results of the analysis of the measured pipe movement provided assurance that the correct design clearances were provided.

A discussion of the strain gauges is provided in Section II.C. The maximum measured fitup displacement of the thermal sleeve relative to the safe end was 0.060 inches. The loads corresponding to this displacement would result in stresses on the order of 60 psi which is negligible in the overall stress evaluation for the safe end to thermal sleeve joint.

The strain gauges also provided a direct measurement of the loads imposed by the recirculation piping on the safe ends. Once again, the low strain values indicated that the safe end loads resulting from the fit up of the piping were low.

Parallel to the efforts of removing the failed safe end-thermal sleeve pieces, a comprehensive program was being conducted to develop qualified manual and automatic machine welding techniques. The techniques included detailed considerations of weld shrinkage to assure the relative position of the new safe end and the thermal sleeve adapter. The relative position of each piece was important to assure the preload values in the original installation were maintained after the repairs were completed.

Each weld was completely mocked up to demonstrate all concerns with respect to radiation protection, procedures, reproducibility of welding and dimensional controls in weld shrinkage. In addition to the above, a comprehensive quality program was developed to cover all facets of the welding program - receiving inspection of welding materials, audits of welding implementation, review of NDE results, audits of housekeeping procedure implementation, audits of cleanliness procedure implementation and corrective action follow up on activities.

After the safe end-thermal sleeve sections were removed, preparations began to do the weld surface preps on the reactor vessel nozzle and thermal sleeve. Once these surfaces were prepared to accept the new thermal sleeve adapter and safe end, the welding process began. The following sequence of operations were performed to complete a nozzle installation:

1. The strain gauge data for cuts #1 and #2 were evaluated, and measurements were taken on the amount and direction of movement of the thermal sleeve after cut #1.

2. Utilizing witness marks to obtain accurate dimensional tolerances, the weld prep's were completed on the thermal sleeve and nozzle respectively. The thermal sleeve adapter could then be welded to the existing thermal sleeve.

3. At this point the new safe end could be fit and welded to the nozzle. After completion of weld #2, the weld gap for weld #3 was measured, and used, in determining the final pre-load condition for the thermal sleeve.

4. Upon establishing the final root gap for weld #3, this weld can be completed. Then both purge gas holes in the thermal sleeve adapter are seal welded.

5. At this time the closure spool piece is templated, and machined, for fitup of the final two closure welds.

6. After welding has been completed on each nozzle, measurements are taken to assure the installation does not impose new design requirements on the piping system.

The safe end welds were subjected to Non-Destructive Examinations according to the following criteria:

1. Radiography in accordance with ASME Section XI, IWA 2231, and with acceptance criteria per ASME Section III, NB 5320.

2. Liquid penetrant in accordance with ASME Section XI, IWA 2222, and with acceptance criteria per ASME Section III, NB 5350.

3. Ultrasonic examination performed to the requirements of ASME Section XI.

Also, all welds associated with the sections of pipe from the recirculation inlet ring header to, and including, the inlet riser elbow will be volumetrically inspected by UT prior to plant startup.

III.E.1 INSERVICE INSPECTION

This section presents the status of the current and proposed Inservice Inspection Program (ISI). The results of the ISI performed at the DAEC for 1976, 1977 and 1978 are also presented. The results of the 1978 ISI include those from the augmented ISI performed in compliance with NUREG 0313.

The present ISI program included in the DAEC Technical Specifications is based on the ASME B&PV Code Section XI, 1971 Edition including the Winter 1972 addenda. Currently under review by the NRC is a revised ISI program for DAEC which is based on the 1974 Edition through the Summer of 1975 Addenda of Section XI of the ASME Code. The proposed ISI program was submitted March 1, 1978 in accordance with 10 CFR 50.55a. Subsequent to a technical meeting with the NRC staff, an amendment to the proposed ISI program was submitted October 13, 1978. The proposed Technical Specification change to conform to 10 CFR 50.55a was submitted to the NRC November 30, 1977. At the present time Iowa Electric does not expect additional NRC questions prior to NRC approval of the proposed ISI program and proposed Technical Specifications. Inspections that will be performed under the proposed ISI program will be augmented in conformance with NUREG 0313.

Under the proposed (revised) ISI program, pressure tests will be in accordance with Section XI of the ASME Boiler and Pressure Vessel Code, and the program period will be from June 1, 1978 through August 31, 1981. The pressure tests will be performed in accordance with procedures which will identify boundaries. The schedule for the pressure test is in accordance with the following table.

ASME Code Class	Test Type	Test Frequency	Test Requirements
	Leakage	After each refueling	IWB-5210 IWB-5221
1	Hydro-static	10 years	IWB-5210 IWB-5222
2	Pressure	10 years	IWC-2412 IWC-2510
3	Pressure	10 years	IWD-2410(b)

The proposed ISI program for the DAEC incorporates the ASME Inservice Testing Program for Pumps and Valves which provides a comprehensive component operability testing plan as required by 10 CFR 50.55a (g). This ASME pump and valve testing program will be in effect as of June 1, 1978, continuing for twenty consecutive months through January 31, 1980. This program is applicable to the safety related, ASME Code Class I, II and III components.

Where testing of an applicable component in accordance with the requirements of Section XI is not possible or is impractical, the proposed ISI program provides the appropriate request for relief, including associated justification(s) and proposed alternate testing requirements.

ISI was performed at the DAEC during the 1976, 1977 and 1978 refueling outages. A special ISI was performed at the DAEC in February 1975 in response to AEC Bulletin 74-10A and NRC IE Bulletin 75-01. All inservice inspections were performed in accordance with the DAEC Technical Specifications.

The 1976 inservice inspection was performed between February 16, 1976, and February 25, 1976, and included an examination of selected reactor vessel, primary system piping, recirculation suction line, and ECCS piping welds. Testing methods included visual, ultrasonic and liquid dye penetrant. No reportable indications requiring repairs or replacement were identified during the outage.

A total of 29 Category "J" welds, 3 Category "D" welds, 2 Category "B" welds were ultrasonically tested. A total of 3 Category "F" welds were ultrasonically and penetrant tested. An additional 15 Category "J" welds were ultrasonically tested on both recirculation suction lines up to the first valve. All welds were visually inspected. Also, the inner radius sections of 3 nozzle-to-vessel junctures were ultrasonically inspected.

The 1977 inservice inspection was performed during the examination of selected reactor welds and components and piping welds and components. Inspection methods included visual, ultrasonic, liquid penetrant and magnetic particle. One indication found on the inner surface and adjacent to a weld in one recirculation bypass line required repair. The repair was made in accordance with qualified and approved procedures.

A total of four Category "B" welds, two Category "C" welds, six Category "D" welds, seven Category "F" welds and 73 Category "J" welds were nondestructively examined. Twenty (20) reactor vessel flange studs and nuts and more than one-third of the reactor vessel flange ligaments between the threaded stud holes were examined. In addition, the inner radius, bore and thermal sleeve welds on all four feedwater nozzles were examined.

The 1978 inservice inspection was performed during the period between March 22, 1978 and April 22, 1978, and included examination of selected reactor welds and components and piping welds and components. Inspection methods included visual, liquid penetrant, and ultrasonic.

One through wall crack was found in the heat affected zone of one weld in the reactor water clean-up system. The crack was found by tracing leaking water to its source. Linear indications were found in an adjacent weld which was removed and replaced with new material. Ultrasonic indications were found in four other welds in the reactor water clean-up system. These welds were radiographed, but the examination did not confirm the ultrasonic indications.

Iowa Electric concluded that the welds were acceptable.

The through wall crack has been analyzed at the Battelle Columbus Laboratory and was found to have been caused by intergranular stress corrosion. In making the repair, five welds were removed and replaced using new Type 316 low carbon stainless steel pipe and a Type 316 stainless steel valve. The new welds were examined by radiography and liquid penetrant and were then examined by ultrasonic for baseline records. The repair was made in accordance with qualified and approved procedures using certified material.

The inner radius and bore of the reactor vessel feedwater nozzles and the control rod drive hydraulic return nozzle were examined. One reactor vessel nozzle to shell weld was examined. The reactor vessel lower head to shell weld, the integral reactor vessel support weld, and two lower head meridional welds were examined. Seventy-nine Category "J" and seven Category "F" pipe welds were examined. Bolting on two valves, three pipe supports, two snubbers, and three restraints in the reactor water clean-up system suction piping were visually examined. No apparent defects were detected in any weld or components other than those found in the reactor water clean-up system pipe welds.

The 1978 ISI results also include the results of the augmented ISI performed at DAEC in compliance with NUREG 0313.

A special inservice inspection was performed in February of 1975 in response to AEC Bulletin 74-10A and NRC IE Bulletin 75-01. This inservice inspection was performed in accordance with the ASME Boiler and Pressure Vessel Code, Section XI and the DAEC FSAR. The examinations were performed by ultrasonic and visual techniques on February 10, 11 and 12, 1975.

Thirty-six welds were examined. Eighteen circumferential piping welds in both loops of the recirculation bypass piping were examined (9 in each loop). Two circumferential pipe welds in one main recirculation piping loop and two circumferential pipe welds on one jet pump riser were examined. Two austenitic

circumferential pipe welds on the control rod drive return system piping were examined. Two welds on the reactor water clean-up system piping were examined. Also examined were four circumferential pipe welds in each core spray piping loop.

All welds were found to be acceptable and no corrective measures were recommended or taken.

III.E.2. Capability of Ultrasonics

Experience gained during the DAEC ultrasonic examinations shows that ASME, Section XI procedures, when applied without baseline data, are capable of detecting cracking greater than 25% of the wall on the .700" thick safe end forgings.

Performing and recording a detailed baseline of the replacement safe ends with the test sensitivity increased beyond ASME, Section XI requirements is expected to enable subsequent similar pressure examinations of the safe ends to achieve a 10% detection level.

III.E.3 INSPECTION OF OTHER INCONEL NOZZLES

A search was made to find other locations on the DAEC Reactor Vessel which contain potentially creviced Alloy 600 material on the primary pressure boundary. The core spray, the feedwater, and the CRD Hydraulic System Return (HSR) nozzle safe ends were the only three locations which contain this condition. Figure III.E.3-1 describes the design configuration for these nozzles and summarizes the maximum stress values at the creviced locations reported in the original vessel stress report prepared by CB&I. A stress index calculation was also completed to determine the susceptibility to IGSCC. The following is a breakdown of the maximum calculated values.

	Stress Index Values				
Nozzle	Primary	Secondary	Peak	Residual	Total
Core Spray	.18	.07	0	.46	.71
Feedwater	.43	.01	.29	.46	1.19
CRD HSR	.10	.20	0	.58	.88

The stress index values for the core spray safe end and CRD return safe end are below 1.0; whereas the stress index for feedwater nozzle safe ends exceeds 1.0. The 1.19 value, however, is significantly less than the 2.24 value calculated for the recirculation inlet safe end and is comparable to the value estimated for the overseas BWR where successful operation was demonstrated for extended service. Also, the feedwater nozzle safe end crevice condition is, in many ways, quite different from that of the recirculation inlet safe end. The crevice in the feedwater safe end is .125 inches maximum as opposed to the 0.50 inch length in the recirculation inlet. Also the pressure boundary material for the feedwater safe end is carbon steel with Ni-Cr-Fe weld metal inlay at the crevice location, whereas, the material in the heat affected zone of the recirculation inlet safe end, where the crack occurred, is wrought Alloy 600. The analyzed weld locations for the core spray and CRD hydraulic system return safe ends are included in the normal inservice inspection program.

The additional inspections planned for the above described nozzle safe ends are as follows:

The carbon steel feedwater nozzle safe end will be examined by ultrasonic inspection techniques prior to restart and during subsequent refueling outages. This examination will include the material adjacent to the Ni-Cr-Fe weld metal inlay at the safe end to thermal sleeve weld.

The core spray and the CRD hydraulic system return line nozzle safe ends will be inspected by ultrasonic inspection techniques prior to restart and each subsequent refueling outage.

The above inspections will continue until such time as industry standards, component configuration changes, or subsequent inspection results dictate revisions to the inspection requirements.

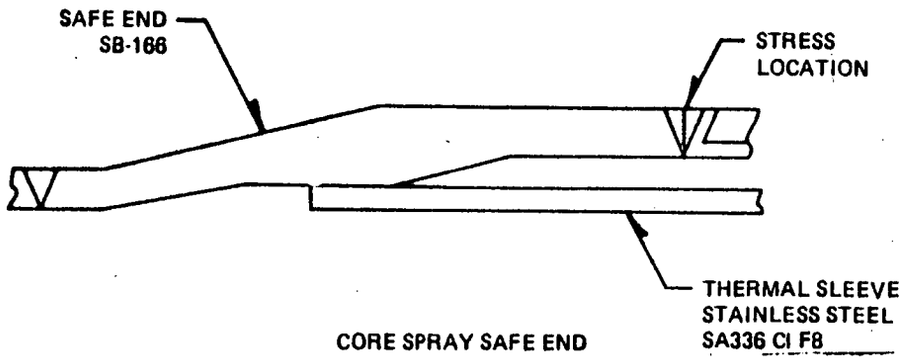

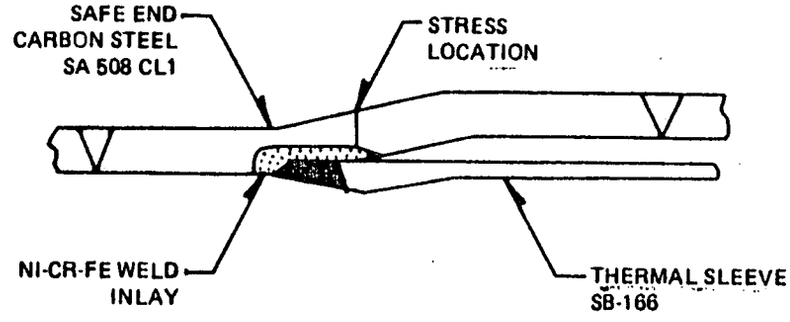

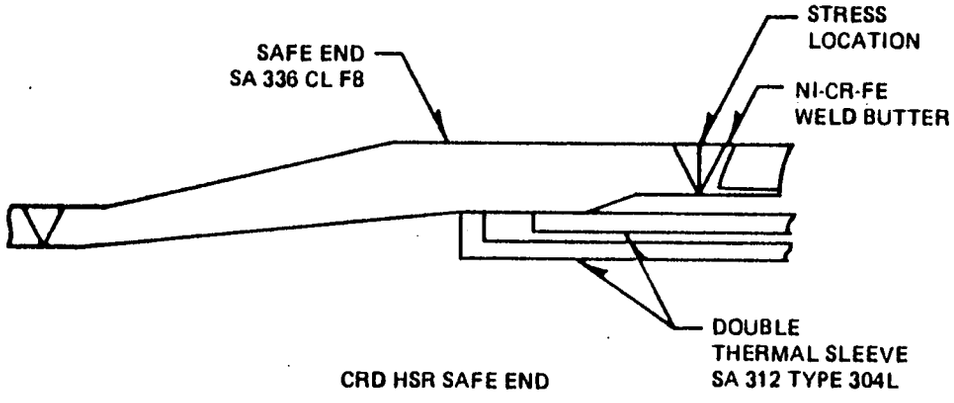

	STRESS CATEGORY	
PRIMARY LOCAL + BENDING (ksi)	PRIMARY + SECONDARY (ksi)	FATIGUE USAGE
13.6	33.5	0.13
15.3	68.4	0.54
9.8	28.8	0.08

Figure III.E.3-1. Maximum Stress Levels

III.E.4. Replacement Safe End Inspections

The N2 safe ends have all been inspected in accordance with design specifications which have been reviewed by Region III I&E inspectors.

A baseline ultrasonic volumetric of the replacement safe ends' pressure boundaries will be conducted utilizing increased sensitivity as described in Section III.E.2. Iowa Electric will conduct an ultrasonic examination of one replacement safe end each refueling outage until all eight safe ends have been examined.